PERFORMANCE EVALUATION OF FOA INTERNAL ENERGY SEPARATORS

R. Whitney, et al

George Washington University

Prepared for:

Office of Naval Research

December 1972

COLUMBIA RESEARCH CORPORATION

AD 764585

PERFORMANCE EVALUATION
OF FOA INTERNAL
ENERGY SEPARATORS

POST OFFICE BOX 485
GAITHERSBURG, MD. 20760

PERFORMANCE EVALUATION OF FOA INTERNAL ENERGY SEPARATORS

Final Report

(3 January 1972 - 30 November 1972)

December 1972

by

R. Whitney
S. Smith

"N0001 9-72-C-0122"

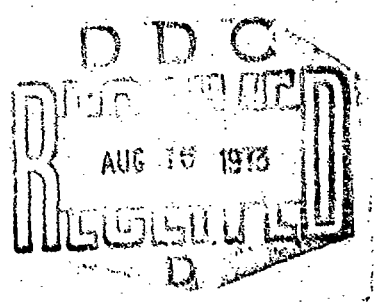

Prepared under Subcontract for
The George Washington University
Washington, D.C.

by

Columbia Research Corporation
Gaithersburg, Maryland

SUMMARY

An experimental test program was undertaken in support of a study by Dr. Joseph V. Foa of The George Washington University. The study concerns the feasibility of utilizing a nonsteady energy separation device to provide conditioned air for aircraft environmental control systems. The results of a theoretical analysis by Dr. Foa indicate that such a device with sufficient cooling capacity for modern military jet aircraft would be much smaller and lighter than the conventional heat exchanger and refrigeration turbine. In order to verify this theory, a model was fabricated and a test program initiated to optimize its configuration. Although the program has not been completed, significant improvements in performance have been achieved by prerotating the inlet air flow and by increasing the portion of the inlet air which is cooled. The device, as presently configured, will provide 10.3 tons of refrigeration per cubic foot of device volume when operating with a 30 psig inlet pressure; which compares favorably with the capacity to volume ratio of current jet aircraft.

Due to the wide operating pressure range in aircraft environmental control systems, a concurrent series of tests was also conducted to determine the effect of various back pressures on the performance of the device. The results of these tests reveal that the effect of back loading is significant; however, it is anticipated that with a proper control system and an improved rotor design, the performance requirements dictated by particular applications can be met.

It is felt that although the current study has verified experimentally that certain design modifications are efficacious, further improvement in the performance of existing models is possible. Specifically, by increasing rotor exit area, improving nozzle design, and utilizing precision machining techniques, a two- to three-fold increase in refrigeration capacity for the same size device should be possible.

TABLE OF CONTENTS

LIST OF FIGURES

LIST OF FIGURES (cont.)

LIST OF TABLES

INTRODUCTION

In military aircraft environmental control systems, cooling air is drawn from two locations -- from the atmosphere as ram air, and from the engine compressor as bleed air. Ram air is used directly to cool unpressurized areas housing electronics and armaments, but pressurized areas such as the cabin must be supplied by higher pressure bleed air. Because it is hot (up to 900°F) as it leaves the engine, bleed air must first be cooled by passing it through a heat exchanger and a refrigeration turbine.

In order to provide an adequate heat sink, many aircraft use heat exchangers weighing hundreds of pounds and taking up many cubic feet of space. Furthermore, at high flight Mach numbers, the stagnation temperature of ram air becomes so high that even these large heat exchangers are inadequate. Problems have also arisen with the expansion turbines used for refrigeration. In late model aircraft, these devices have rotational speeds of 70,000 to 80,000 rpm, and as a result, have a very low Mean Time Between Failure (e.g., 500 hours in the latest attack bomber). The cooling needs of both subsonic and supersonic aircraft must, therefore, rely on fragile and increasingly larger equipment.

An alternative to the current equipment is the Foa Energy Separator (FES).[1,2] This device essentially provides its own heat sink by separating input air into two streams; removing energy in the form of heat from one stream and adding it to the other. Thus, both hot and cold output flows emerge, and because the process is isentropic, high efficiencies are possible. The principal advantages of the FES over current systems include a significant reduction in weight and volume through the elimination of heat exchangers, and an increased Mean Time Between Failure by

the replacement of the expansion turbines.

To investigate these advantages, the Naval Air Systems Command has contracted with The George Washington University to:

1. theoretically analyze the various FES configurations;
2. predict size and weight reductions possible for a specific aircraft;
3. predict heat sink substitute capacity; and
4. evaluate the actual performance of model energy separators, including a variable geometry device fabricated specifically for this purpose.

This report details the work performed by Columbia Research Corporation (CRC) (in accordance with item 4 above) under a subcontract to The George Washington University. Tests were conducted on a single rotor energy separator with fixed geometry and a double rotor energy separator with interchangeable collectors and center sections. The latter device is referred to as the "variable geometry model". Test results are presented in graphic form and evaluated to reveal preferred FES geometry. Fabrication and test procedures are also outlined.

ENERGY SEPARATOR OPERATION

The principles of operation of the energy separator can be explained with reference to Figure 1.[3] Consider a jet issuing from a nozzle inclined at an angle β to the horizontal. The jet impinges on a wall and splits into two streams designated in the figure as 'h' and 'c'. Due to the inclination of the jet, the streams do not divide equally, but the majority of the flow is diverted to the 'c' side. This is a steady flow condition and assuming negligible viscous losses, the temperatures of the two streams are equal to the temperature of the main jet. If the jet and wall are suddenly set in motion at a velocity, V, in the direction shown in Figure 1, then this velocity must be added vectorially to the stream flow velocities, U_c and U_h, with the result that the velocity of stream 'h' is increased and the velocity of stream 'c' is decreased.

In effect, what has occurred in this process is a transfer of energy in the form of flow velocity from stream 'c' to stream 'h' without any external work being done. If the streams are brought to rest in separate chambers, their kinetic energies, due to the flow velocities, will be converted to internal energy. The rise in the 'h' stream internal energy is greater than the rise in the 'c' stream internal energy since the 'h' flow velocity is greater than the 'c' flow velocity. Temperature is related directly to the internal energy of the gas, and therefore, each chamber will be at a different temperature. In particular, the chamber temperature on the 'c' side will be lower than the inlet temperature, and the temperature on the 'h' side will be higher. The magnitude of the temperature changes is a function of the mass flow rates of the streams, with the 'h' stream temperature rise being greater than the 'c' stream temperature drop due to the lower flow on the 'h' side.

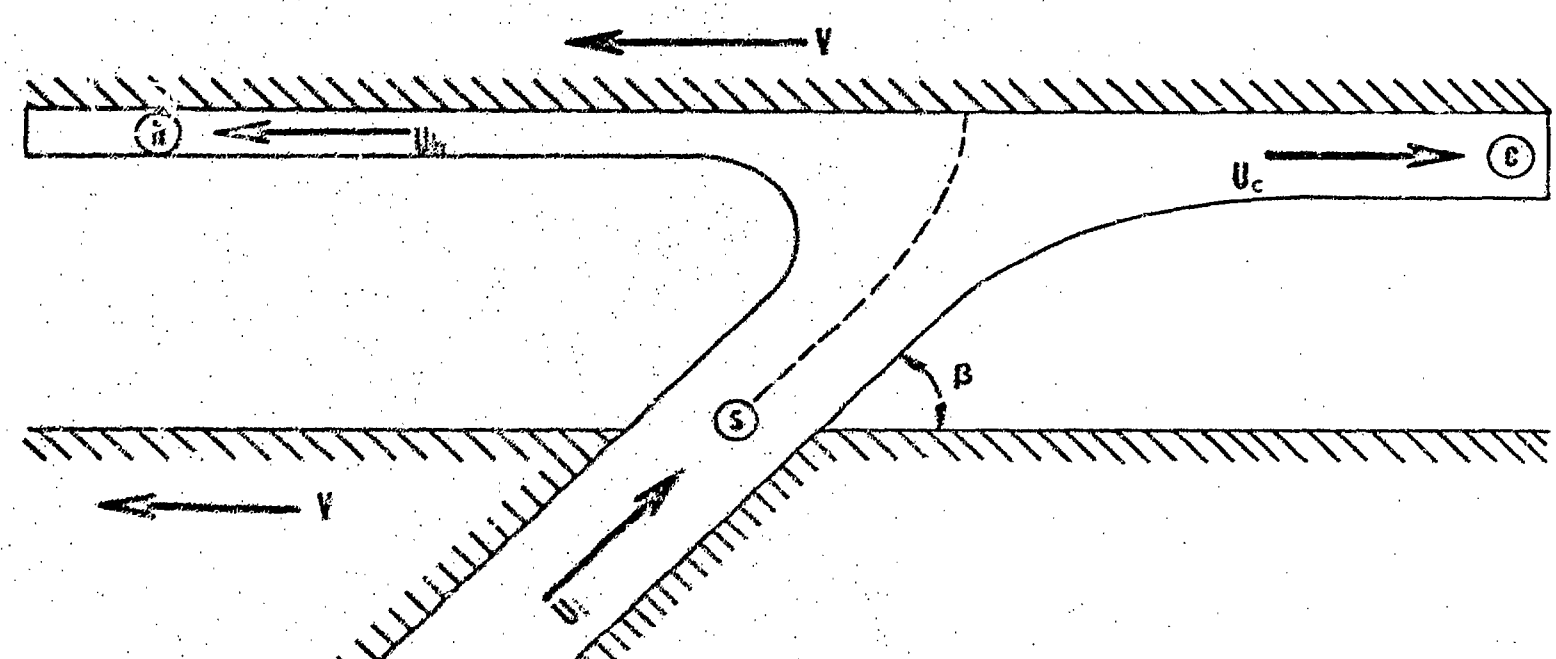

FIGURE 1. A SCHEMATIC OF THE ENERGY SEPARATOR IN ITS SIMPLEST CONFIGURATION

The physical phenomenon which causes energy separation occurs at the stagnation streamsurface between the two flows, designated 's' in Figure 1. The pressure forces acting at this interface are in motion when the system is in motion, and therefore positive work is being done by the 'c' stream and negative work is being done by the 'h' stream. Thus, energy is transferred from 'c' to 'h'.

Several energy separator configurations have been developed. These are classified as either external or internal separation devices, depending upon where the stream separates relative to the jet driver. In external separation, as depicted in Figure 2 (from Ref. 1), the radially flowing jet is separated into high and low temperature streams external to a driving rotor. This is similar to the arrangement shown in Figure 1, except that the motion is rotational rather than translational. In internal separation, as shown in Figure 3 (from Ref. 1), the streams are separated within a rotor by means of opposing sets of nozzles located in different axial rotor planes. One set of nozzles has larger throat areas and, consequently, the rotor rotates opposite to the direction of these issuing jets, thereby producing the motion required for energy separation.

Each flow separation configuration offers certain advantages and disadvantages. The external energy separator, for example, is the easiest to fabricate; however, the collection losses and sensitivity to back pressure variations may reduce the efficiency of the device. On the other hand, the internal energy separator is less sensitive to back pressure variations, and collection losses can be reduced by proper design of the outlet chambers; however, rotor construction is more difficult due to the requirement for

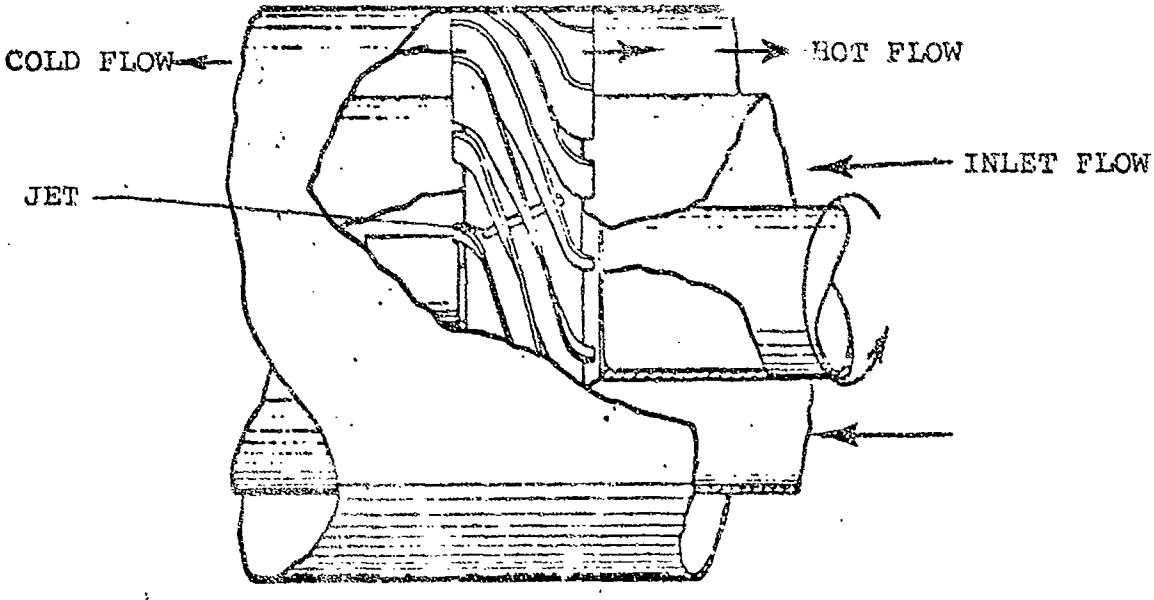

FIGURE 2. AN EXTERNAL ENERGY SEPARATOR CONFIGURATION WITH ROTOR MOUNTED TURNING VANES

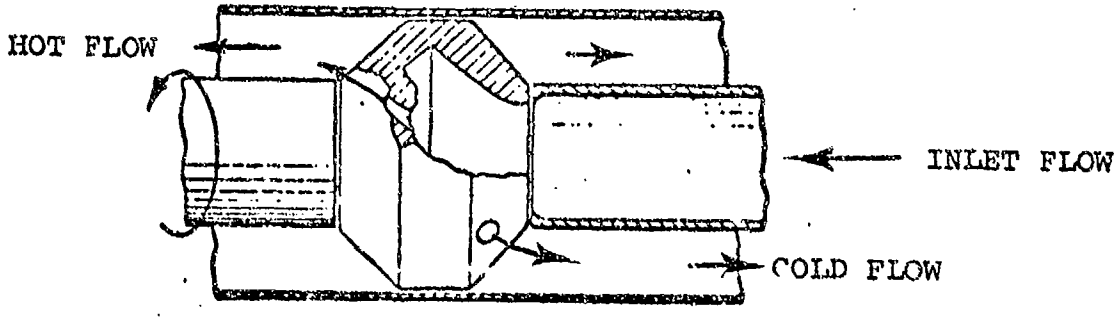

FIGURE 3. AN INTERNAL ENERGY SEPARATOR CONFIGURATION WITH A SINGLE ROTOR

precisely shaped nozzles to reduce the entrance losses. Any determination of which configuration is best for aircraft applications must be prefaced by a detailed study of each. The present study is concerned only with the internal energy separator primarily because of the availability of two rotors, and is not an indication of any a priori preference for this configuration.

SINGLE ROTOR INTERNAL ENERGY SEPARATOR

Introduction

Preliminary to the fabrication of a variable geometry internal energy separator, a fixed geometry model was tested to assess the importance of various design factors and, in general, to gain a working knowledge of the energy separator concept. The device used for this study was originally designed and fabricated at Rensselaer Polytechnic Institute (RPI) for a previous test program.[4]

The RPI model has a single rotor which is supported by a cantilevered shaft. Air is supplied to the rotor along the axis of rotation on the side opposite the shaft. The air issues from a pipe and expands into the rotor cavity. The rotor is composed of the cavity and two sets of nozzles, each directed so as to produce rotation of the rotor in opposite directions. There are two nozzles in each set. One set has throat areas larger than the other, and consequently the jets issuing from these nozzles have a larger angular momentum. It is this set that determines the rotational direction. The nozzle sets are separated axially along the rotor and the flows issuing from them are prevented from mixing by the collector housing. For the reasons described previously in the section on energy separator operation, the temperatures of the air discharged from each set of nozzles are different; in particular, the driving nozzle set discharge air temperature is lower than the inlet temperature and the driven nozzle set discharge air temperature is higher than the inlet temperature.

Unfortunately, the RPI model was delivered to Columbia Research Corporation (CRC) in damaged condition, necessitating repairs to

the collector housing, base plate, and rotor. The collector housing was completely destroyed, requiring the fabrication of a new housing. This was particularly difficult because there were no detail drawings of the device, and dimensions had to be determined directly from the damaged piece. The base plate was bent slightly, which prevented the alignment of the rotor and the collector housing; therefore, a new plate had to be fabricated before proper alignment was achieved. Finally, the rotor had to be cylindrically ground to remove scored areas on the periphery. The repaired model is shown in Figure 4 (see Ref. 4 for comparison with original RPI model).

Even after the model was repaired, however, its performance was significantly less than in earlier tests at RPI with the original model.[1] The rotational speeds were considerably lower than anticipated, due primarily to a defective bearing which greatly increased restraining torque on the rotor. It was, therefore, decided to redesign the bearing housing and replace the bearings. The new bearing housing attached directly to the collector housing, eliminating the rotor-collector alignment problems and allowing the convenient insertion and removal of the rotor. With the new bearing arrangement, rotational speeds above 50,000 revolutions per minute were obtained. At these high speeds, however, a slight asymmetry in the rotor caused large amplitude vibrations, necessitating dynamic balancing of the rotor. These modifications significantly improved the performance of the model.

Model Construction

An assembly drawing of the energy separator is shown in Figure 5. The base is fabricated from 1-inch thick steel plate milled flat to allow the proper alignment of the inlet pipe and the rotor cavity. The inlet pipe is standard 3/4-inch diameter galvanized steel with two instrumentation taps; one for an inlet

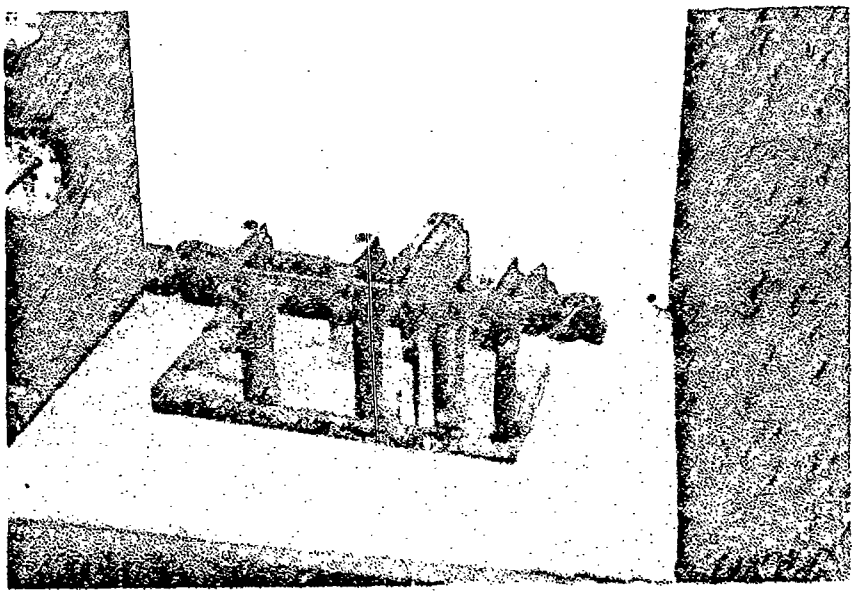

FIGURE 4: SINGLE ROTOR INTERNAL ENERGY SEPARATOR IN ORIGINAL CONFIGURATION AFTER REPAIRS.

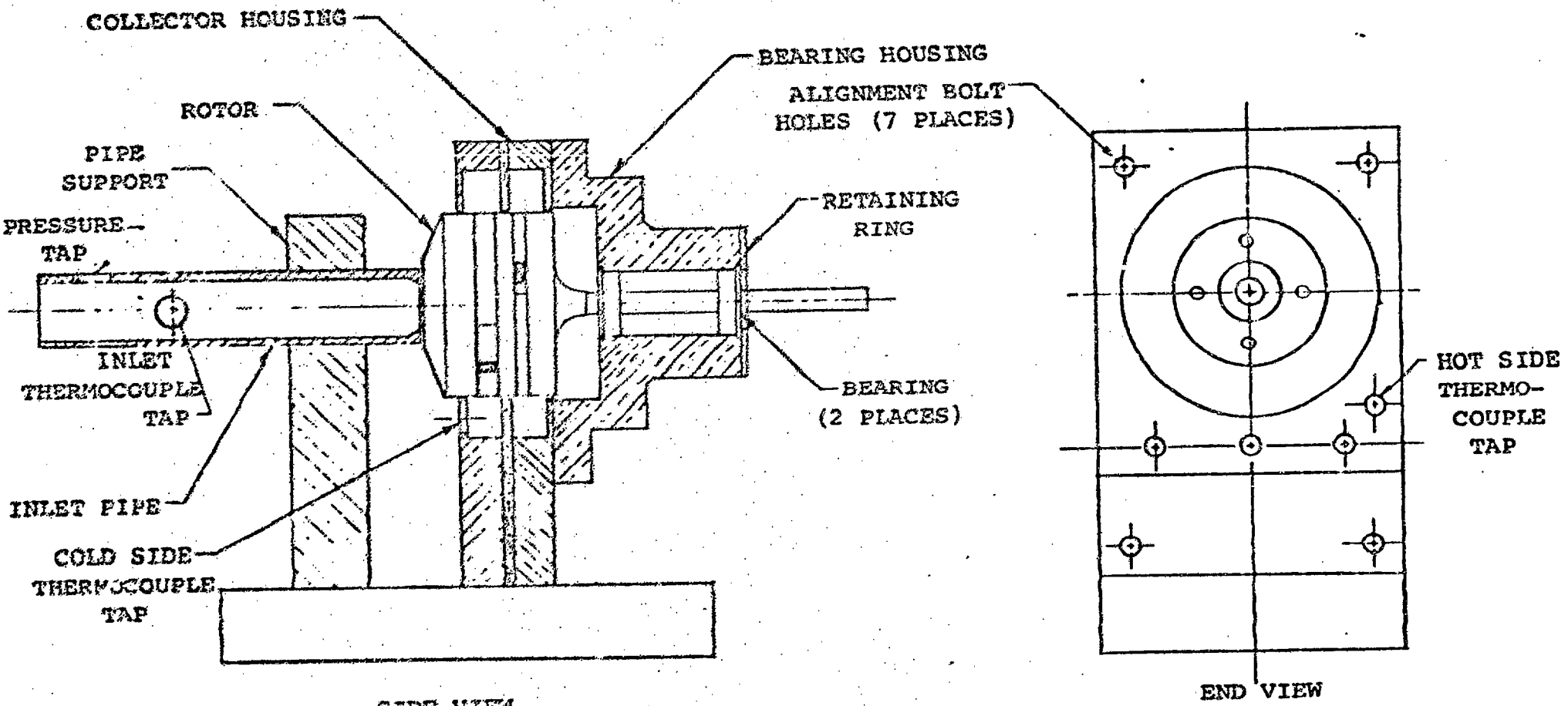

FIGURE 5. ASSEMBLY DRAWING OF A SINGLE ROTOR INTERNAL ENERGY SEPARATOR AS MODIFIED BY COLUMBIA RESEARCH CORPORATION

static pressure probe and the other for an inlet temperature thermocouple. The pipe is modified somewhat by the insertion of a slight constriction at the exit plane, which reduces the flow loss as the air jet expands in the free space between the pipe and the rotor cavity inlet. This design feature, a part of the original RPI model, has been found to be very effective and, in fact, at certain inlet pressures, the air jet actually aspirates ambient air into the rotor cavity. However, to reduce flow losses at all inlet pressures, the clearance between the pipe and the rotor is kept to 0.010 inches by adjusting a clamp on the pipe support. To insure that the rotor is not scored by an accidental jarring of the device during operation, the end of the pipe is coated with a tough epoxy coating powder, manufactured by Armstrong Products Company, which acts as a buffer to prevent direct contact of the metal parts.

The collector housing is fabricated in three sections. The two outer pieces are made of aluminum and contain the annular flow collection spaces; the middle piece, made of nylon reinforced phenolic, prevents the mixing of the air issuing from the two sets of rotor nozzles. In addition to acting as a physical barrier between the flows, the phenolic center section is also a thermal insulator, preventing the transfer of heat from the hot side collector to the cold side collector. The collector has thermocouple taps near each exit to allow measurement of rotor nozzle exit temperatures.

The rotor fits into the collector housing so that the nozzles are aligned within their appropriate collectors with a clearance between the rotor outside diameter and the housing internal diameter of 0.010 inches. A sandwich construction is used for the rotor, with the nozzles consisting of aluminum plates

bounded by three stainless steel plates. The front plate contains the rotor cavity inlet port; the middle plate, a large annular cut-out forming the rotor cavity; and the end plate, a slightly undersized shafting hole. The shaft was secured to the end plate by heating the area around the undersized shafting hole until itexpanded sufficiently to allow the insertion of the shaft. After cooling, the shaft and plate were permanently bonded together. The entire rotor was assembled with alignment screws and 'trued' between centers on a cylindrical grinder. The rotor was then dynamically balanced to within the accuracy dictated by the bearing tolerances.

The bearing housing is constructed entirely of stainless steel and attaches directly to the collector housing by means of five bolts. Two identical shielded deep groove radial ball bearings with rated rotational speeds of 48,000 rpm are included within the assembly. The radial play of these bearings 0.0002 to 0.0004 inches, is the limiting factor in rotor balance mentioned previously. To facilitate removal of the rotor from the housing, the bearing bore is sized to allow a 0.0001- to 0.0003-inch clearance fit between the bearing and the rotor shaft.

The previously described modifications to this model allowed its testing to rotational speeds limited only by the rated bearing speed. Operation above the 48,000 rpm is possible; only, however, with a significant sacrifice in bearing operating life. The modified device is shown in Figure 6.

Test Program

Testing of the single rotor internal energy separator was conducted primarily for the purpose of evaluating the various design modifications, since its construction did not allow for the investigation

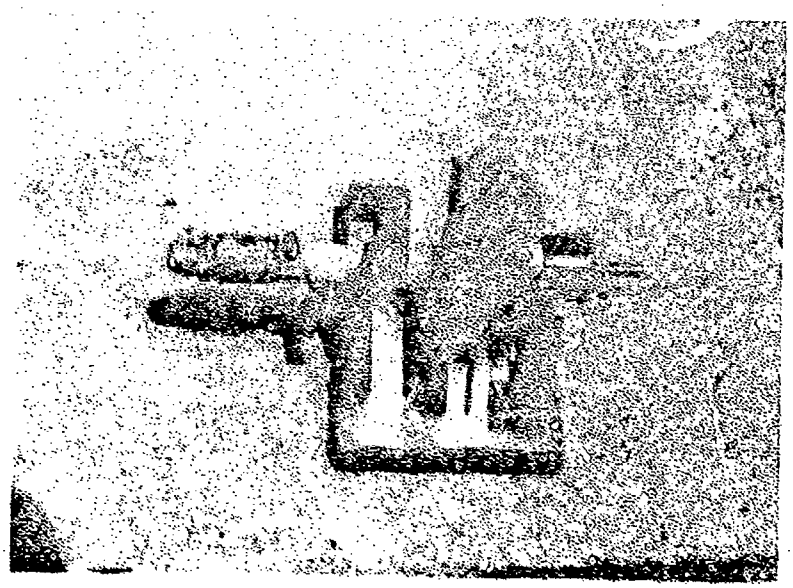

FIGURE 6: SINGLE ROTOR INTERNAL ENERGY SEPARATOR AS MODIFIED BY COLUMBIA RESEARCH CORPORATION.

of the effects of changes in device geometry and back loading. As changes were made, the device was tested to determine the corresponding improvement in performance. Primary consideration in this regard was given to the increase in rotational speed of the rotor at a given inlet pressure, since it was known from theory that the higher the peripheral velocity of the rotor, the greater the energy separation. The improvement in performance was particularly significant after installation of the new bearing housing, when the rotational speed at 45 psig inlet pressure increased from 23,400 rpm with the old housing to 48,420 rpm with the new, and the output temperature difference increased from 88°F to 133°F.

Results of a test on the device in its final configuration have been tabulated in Table 1. All temperatures were measured with iron-constantan thermocouples and displayed on a Model 1602 Comack Thermometer. The thermocouples were mounted at the inlet and outlets of the device as noted on the assembly drawing (Figure 5). The rotational speeds were measured with a Model 510-AL Sticht Stroboscope and were an average of several readings, since the condensation of moisture within the device could cause speed fluctuations of $\pm$ 500 rpm.

In general, it can be said that the redesigned device performed well mechanically, although the energy separation obtained was less than in earlier tests at RPI with the original model. Further improvements to the device, such as decreasing clearance between the rotor and the collector housing to reduce mixing between the outlet flows, increasing the shaft diameter to prevent slippage, and improving nozzle entrance geometry would have undoubtedly increased the device efficiency. These deficiencies were not corrected, however, since knowledge of these defects could be applied to the design of the variable geometry model.

Rotor Speed (RPM)	Temperature (^{o}C)			Temperature Difference (^{o}F)
	Inlet	Cold	Hot	
31,070	18	2.5	40.5	68
38,150	18	-2	49	92
46,558	20	-6	59	117
48,420	21	-9	65	133

TABLE I. TEST RESULTS FOR THE SINGLE ROTOR INTERNAL ENERGY SEPARATOR.

VARIABLE GEOMETRY ENERGY SEPARATOR

Using preliminary data from single rotor energy separator tests, the design of a variable geometry FES was undertaken. The device was constructed so as to permit changes in three parameters; back pressure, area ratio, and prerotation. Back pressure, defined as the pressure seen at the output face of the rotor, can be expected to vary in operational devices due to fluctuating demands for heated or refrigerated air downstream. During testing, however, the back pressures in both exit chambers were kept equal. Unlike back pressure, area ratio and prerotation should not change during operation, but are design variables whose effects must be understood to maximize energy separator performance. In internal separation devices, area ratio determines the percentage of flow to each side and ultimately the overall performance of the device. Prerotation is defined as an angular velocity in the direction of rotor movement imparted to the incoming air. Its proper use will enhance performance of an energy separator in any configuration. An examination of the individual and collective effects on internal energy separator performance of these three variables is the object of this portion of the study.

Model Construction

Rather than design a completely new internal energy separator, it was decided to incorporate features into an existing model which would allow the interchange of several components. A dual rotor device, designated Model III, was made available by the principle investigator, and the initial effort was centered around modifying it for use in the program. In its original state, Model III used two rotors mounted about 2½ inches apart on a short shaft (Fig. 7). One rotor contained four cold flow nozzles with a combined area of .336 square inches. The other contained four hot flow nozzles with a

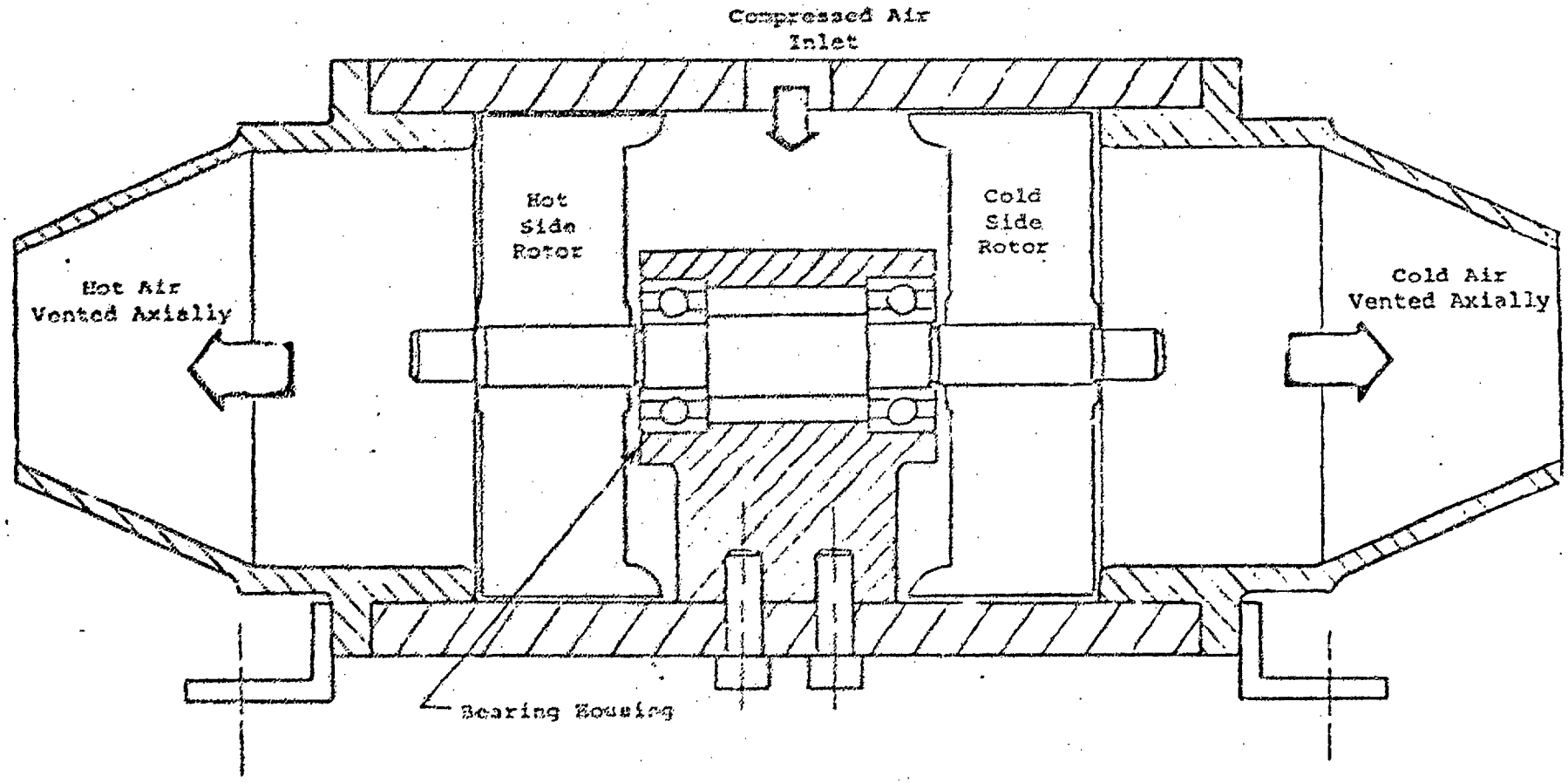

FIGURE 7. SECTIONAL VIEW OF ORIGINAL MODEL III ENERGY SEPARATOR GEOMETRY.

combined area of .194 square inches. The rotors, supported on ball bearings mounted between them, turned within a cylindrical housing. A thick pedestal connected the outer casing and the bearing housing. In this manner, a small clearance could be maintained between the rotors and their casing. Compressed air introduced between the rotors passed through the nozzles and was vented axially. Because the outlet flow was unobstructed, there was a substantial noise reduction over the single rotor model, but the central bearing support seriously disturbed the incoming air and detracted from performance of the model.

In order to provide a smooth entrance flow, it was suggested that the supporting pillar be replaced with a spiral fence (Fig. 8). As entering air struck the bearing housing, it would split into two flows. The spiral fence would then keep the flows separated and cause them to acquire an angular velocity (prerotation) as they turned about the bearing housing and entered the rotors. Varying the pitch and direction of the fence would permit variations in the degree and sense of the prerotation. It was necessary, however, to design a fence rigid enough to replace the supporting pillar.

Due to the close rotor clearances required for optimum performance, only minute deflections of the rotors could be allowed. A stress analysis performed for the existing Model III has shown that the attachment to the outer casing must be exceedingly rigid. This would require considerable precision machining and alignment. Anticipated problems in producing such a support led to further modification of the design.

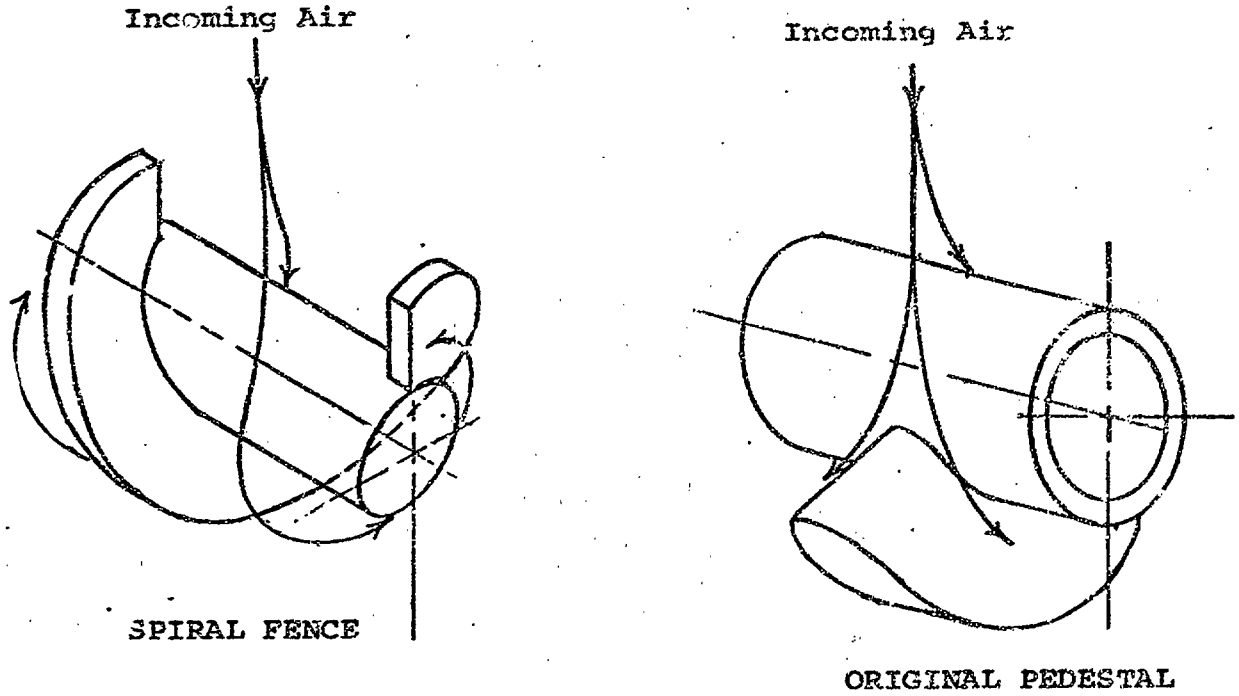

FIGURE 8. MODIFICATION OF BEARING SUPPORT.

It was noted that moving the bearings from the center to the ends of the shaft would eliminate all structural loads on the spiral sections. Simpler production and attachment methods were then devised, permitting use of several different prerotations in the test program at reasonable cost. End bearings, however, would interfere with the exit flow unless collectors were added to turn the air as it left the rotors and vent it radially.

The collectors were designed in three layers, as shown in Figure 9. The outer parts (one on each end) formed the backs of the collectors and contained the bearings. The middle sections contained collection channels of increasing radii, terminating in vents. The inner sections formed the fronts of the collectors, and when welded to the cylindrical outer casing, served to locate the other two. Using this construction, the outer sections, with their closely machined bearing mounts, could be left unchanged, while different middle sections could be installed to alter back pressure or other collection effects.

These changes in the Model III design, necessary to produce a variable geometry energy separator, required reconstruction of the device except for the rotor. Relocation of the bearings necessitated construction of a new shaft and outer casing. The hot side rotor was pressed onto the shaft, but the cold side was keyed and held on with a cap and screw to permit its removal and facilitate changes in prerotation geometry. After early testing, it was also necessary to install a cap and screw to secure the hot side rotor, which tended to slip at high rotational speeds. Before installation, the rotor-shaft assembly was dynamically balanced. The new outer casing was made to allow for the reduced distance between

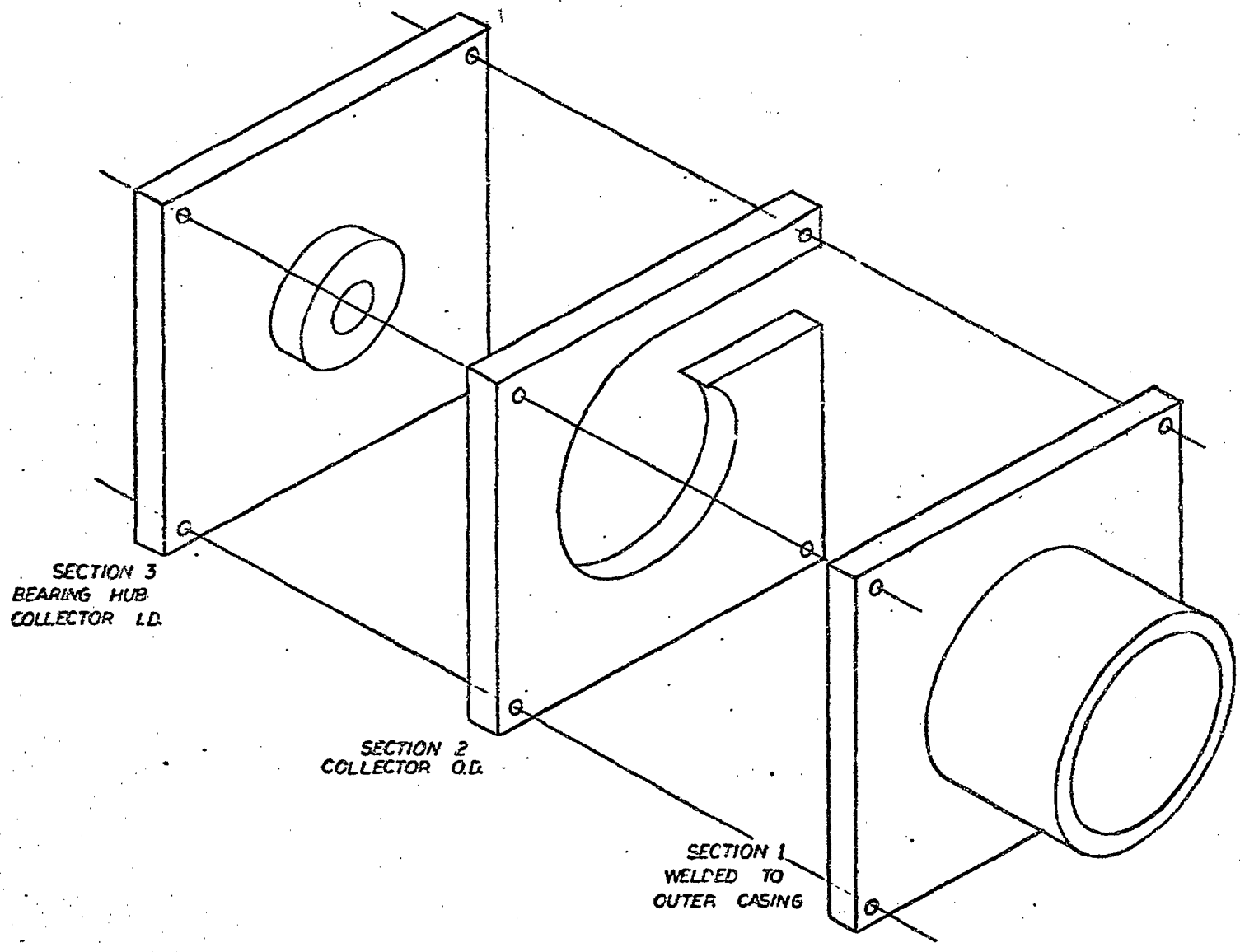

FIGURE 9. LAMINATED CONSTRUCTION OF END PLATE COLLECTORS FOR THE VARIABLE GEOMETRY ENERGY SEPARATOR.

rotors, to accept an aircraft type V-band inlet fitting, and to permit attachment of the end plate collectors. The final configuration is shown in Figure 10.

Middle section collector plates with four different geometries were constructed for each side. The effects, however, were not found to be sufficiently repeatable for use in the test program. A single collector geometry for each side was therefore selected, providing 2.50 square inches of vent area to the cold side, and .375 square inches of vent area to the hot side. Ducting was mated to the collector vents and valves installed to restrict the outlet flow as required to change the back pressures. This arrangement provided fully repeatable data points without requiring disassembly of the device.

In order to determine the effect of different nozzle area ratios, it was proposed that the hot side nozzles be partially blocked. Reducing the area of all four nozzles would have reduced the nozzle efficiencies and necessitated rebalancing of the rotors. It was decided, however, to use only two area ratios, one with all four hot nozzles open, and one with two nozzles totally blocked and two open. This was accomplished by filling two nozzles 180° apart with equal amounts of epoxy. The result was a new area ratio without any major effect on the rotor balance.

Test Program

The two area ratio configurations were used in the test program in each of three prerotation modes. One provided no prerotation; another provided positive (i.e., in the direction of rotor movement) prerotation to the cold side and negative (i.e., opposite to rotor movement) prerotation to the hot side; and the third provided negative prerotation to the cold side and

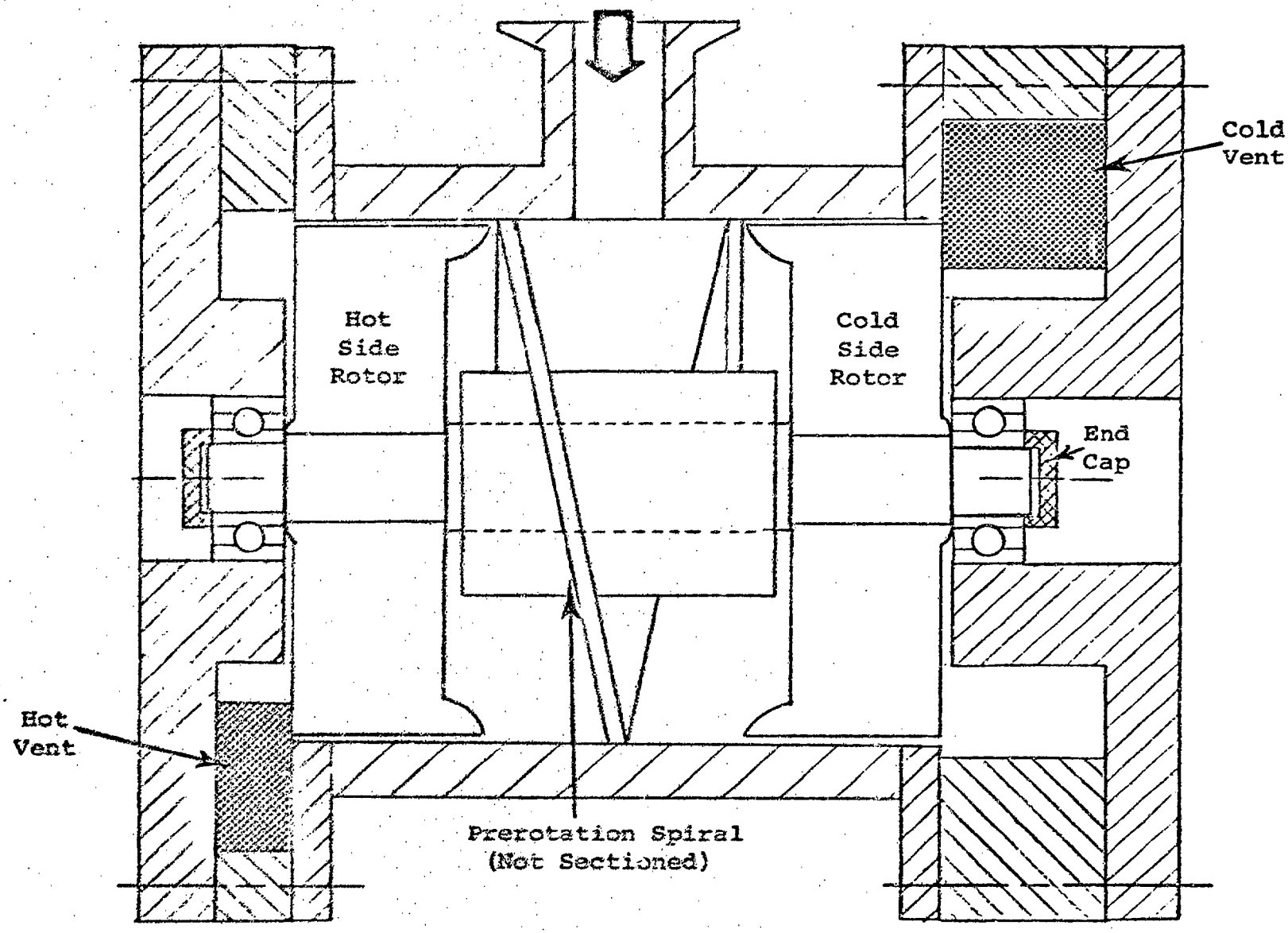

FIGURE 10. FINAL CONFIGURATION FOR MODEL III, VARIABLE GEOMETRY FOR ENERGY SEPARATOR.

positive to the hot. Each of these six configuratio.s was tested at a series of inlet pressures (2, 5, 10, 20, 30, and 40 psig) and with the back pressure varied between 0% and 50% of the inlet pressure. The back pressures at the hot and cold exits were varied simultaneously. Between 12 and 16 pressure combinations were investigated for each configuration, with two or three sets of measurements at each point. The measurements taken included pressures, temperatures, rotor speed, and flow rates. Pressure readings included both inlet and outlet (i.e., back pressure) on each side, and were taken with Bourdon tube gauges. Temperatures were measured with iron-constantan thermocouples and read on a Comark Thermometer and on Omega millivolt meters. Five locations were monitored, including inlet, and two points each on the hot and cold sides. Flow rates were measured at the inlet by means of an Annubar 700 series flow meter. Tables of data taken are presented as Appendix I.

Results

During the course of the test program, the effects of back pressure, prerotation, and area ratio were examined in every possible combination. In no instance was an interrelated effect noted. Examining the three individually, back pressure (equal for both outlets) can be said to have no effect on either rotational speed or temperature differential, provided that the inlet pressure is modified to provide a constant pressure ratio. Both area ratio and prerotation, however, have significant effects on these parameters.

By reducing the area ratio, the percentage of inlet air expelled from the cold nozzles (cold fraction) is increased. As a result, more power is available to spin the rotor, resulting in high rotor velocities and greater temperature differentials.

Also, because the energy removed from cold side must be absorbed by a smaller mass hot air, the hot side temperature increases dramatically. This effect may be noted by comparing the graphs in Figure 11 with those in Figure 12. The area ratio .577 results in a nominal cold fraction of .63. Reducing the area ratio to .289 increased the nominal cold fraction to .77, resulting in nearly doubled rotor speed and temperature differential. At a given rotor speed, however, the total temperature differential is about the same (Figure 13), being slightly greater on the hot side and slightly less on the cold side for the smaller area ratio. The penalty paid for greater energy transfer, therefore, is an increase in rotor speed and corresponding structural difficulties.

Unlike modifying area ratio, providing proper prerotation can increase temperature differentials without increasing rotational speed. Comparing Figures 11a and 12a with 11b and 12b, respectively, shows that, at a given pressure ratio, positive prerotation to the cold side and negative prerotation to the hot side increase energy transfer significantly. Figures 11c and 12c show that reversing the prerotation produces a lesser energy transfer. The increased temperature differential with positive prerotation occurs despite a reduction in rotor speed, as shown in Figure 14. Graham[3] suggests that prerotation may slightly alter the cold fraction and, thus, the power available to the rotor. Fortunately, the actual change in temperature differential caused by prerotation is quite large at a given rotational speed (see Figure 15), and apparently overshadows the reduction in rotor speed at a given pressure ratio.

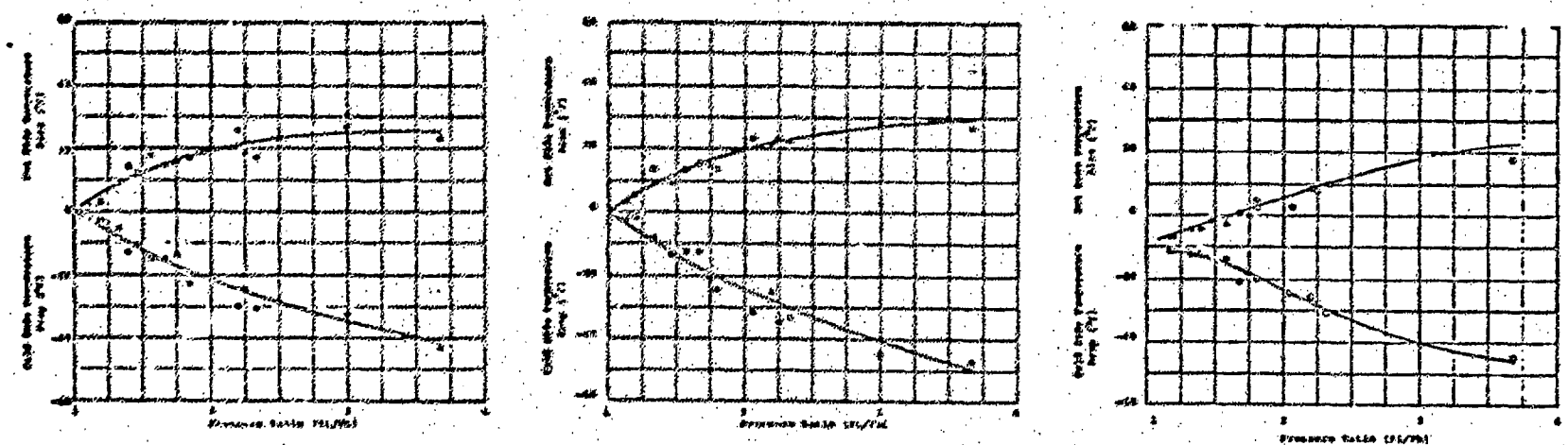

(a) No Center Section

(b) Positive Cold Side Prerotation

(c) Negative Cold Side Prerotation

FIGURE 11. EFFECT OF PRESSURE RATIO ON ENERGY SEPARATION WITH A NOZZLE AREA RATIO OF 0.577.

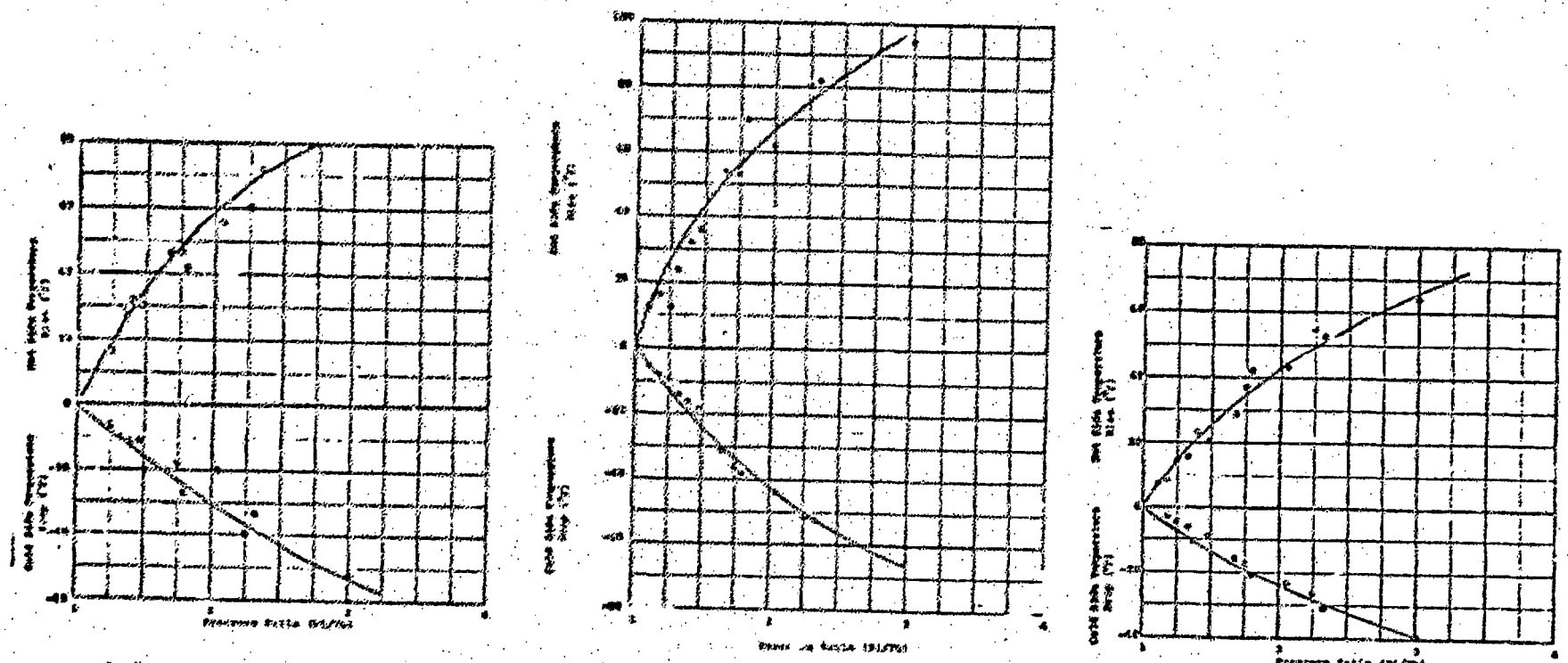

(a) No Center Section

(b) Positive Cold Side Prerotation

(c) Negative Cold Side Prerotation

FIGURE 12. EFFECT OF PRESSURE RATIO ON ENERGY SEPARATION WITH A NOZZLE AREA RATIO OF 0.289.

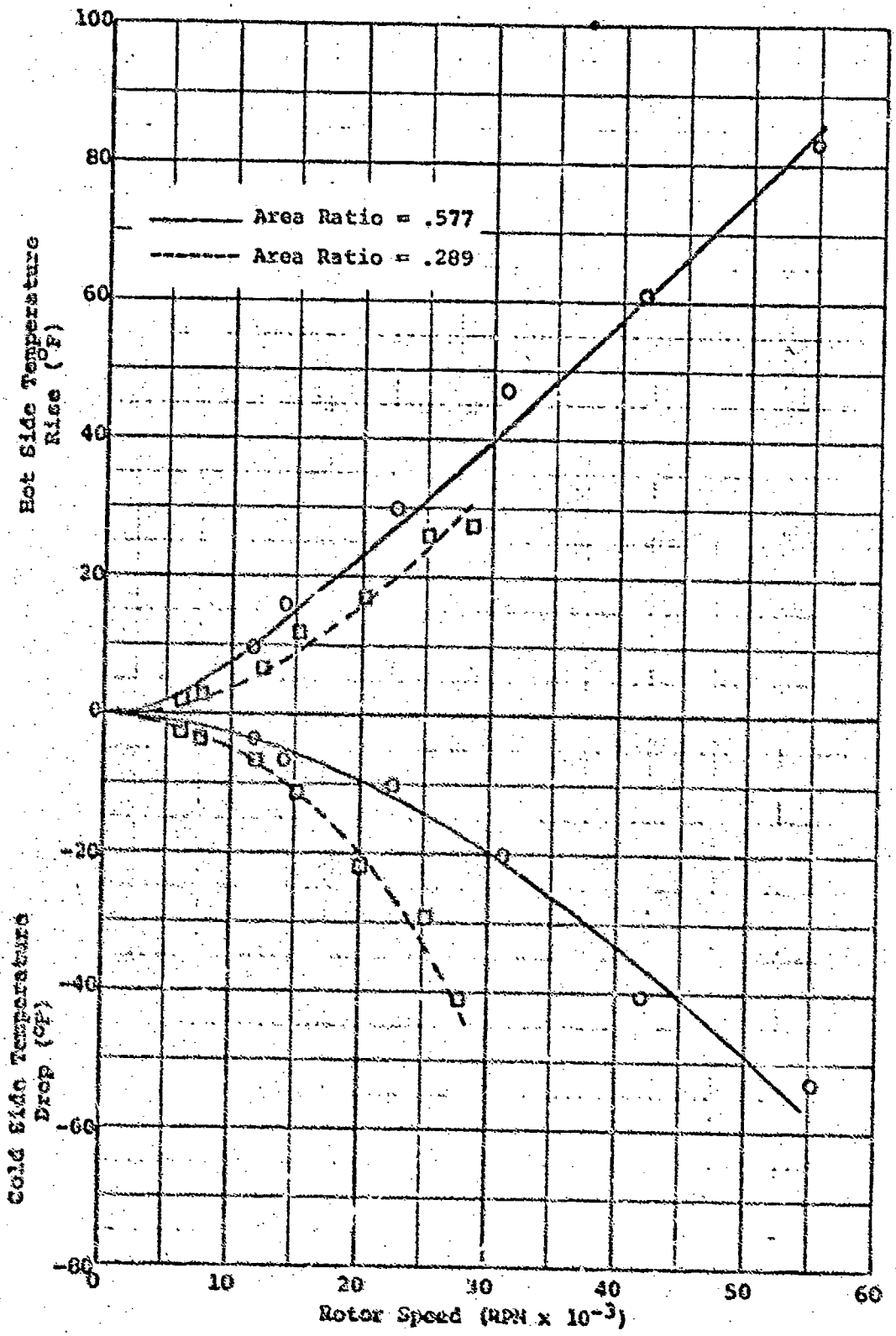

FIGURE 13. EFFECT OF AREA RATIO ON ENERGY SEPARATION FOR AN FES-3 CONFIGURATION WITH NO PREROTATION.

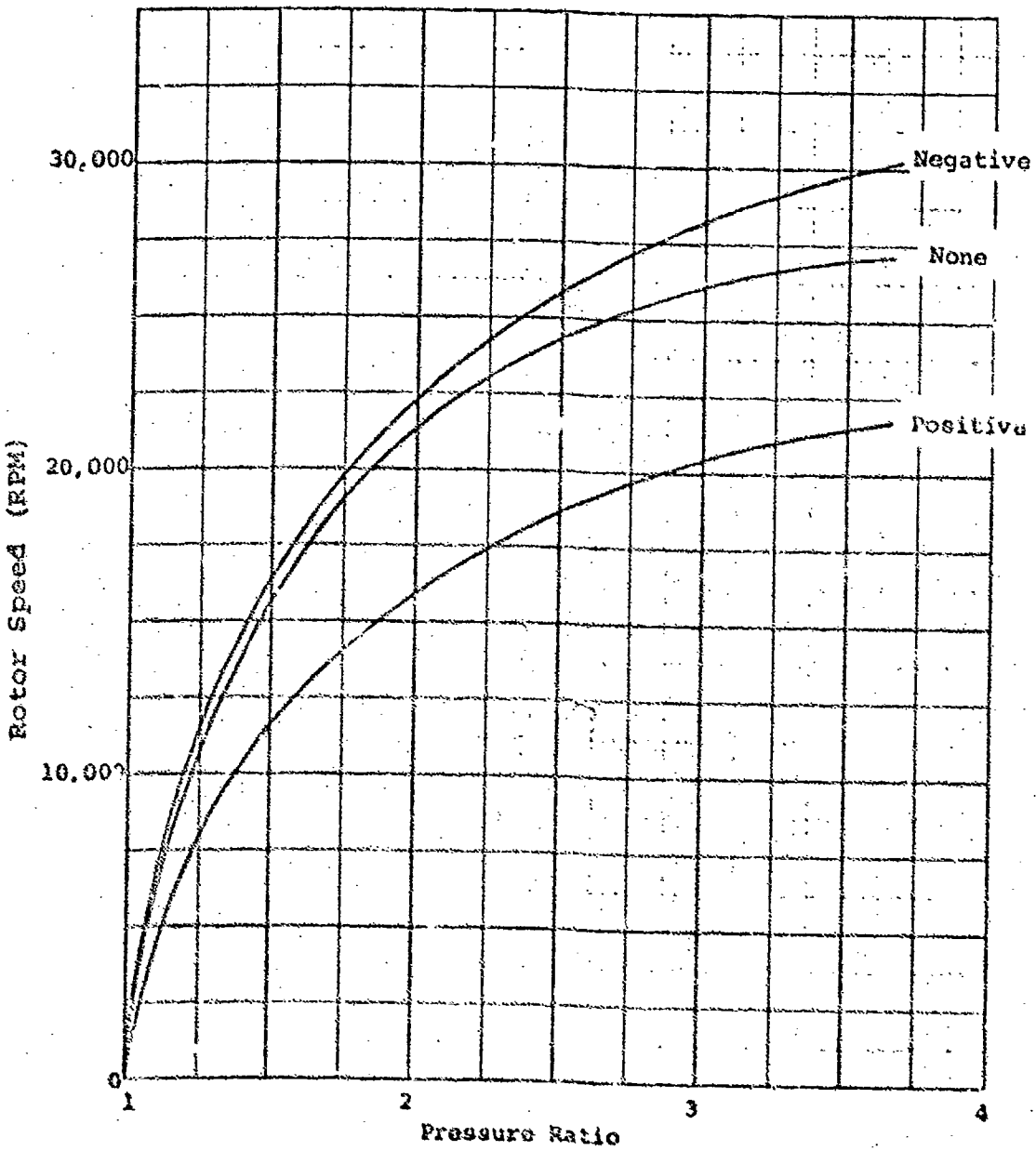

FIGURE 14. EFFECT OF COLD SIDE PREROTATION ON ROTOR SPEED FOR AN FES-3 CONFIGURATION WITH AN AREA RATIO OF 0.577.

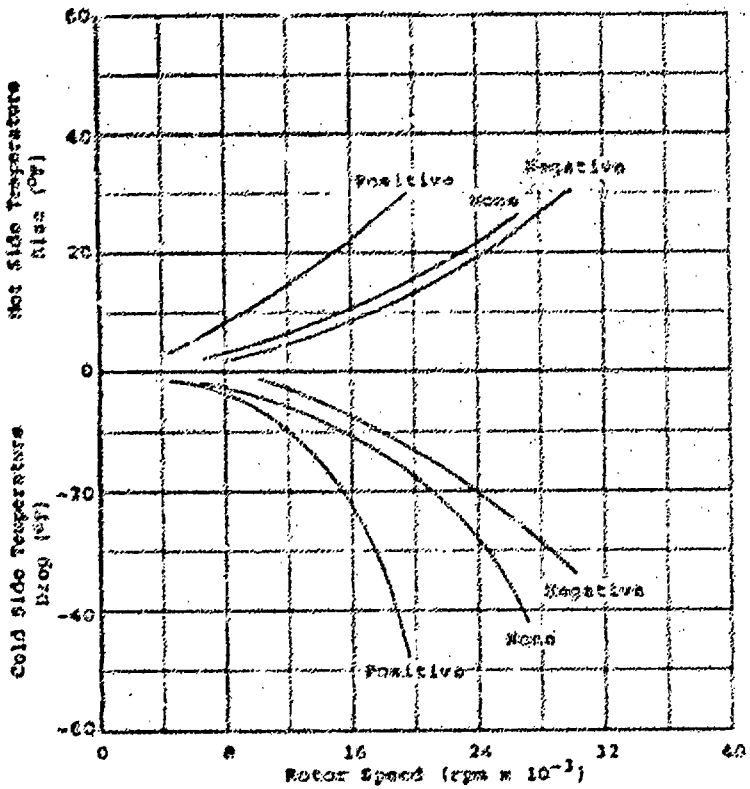

(a) 0.577 Area Ratio

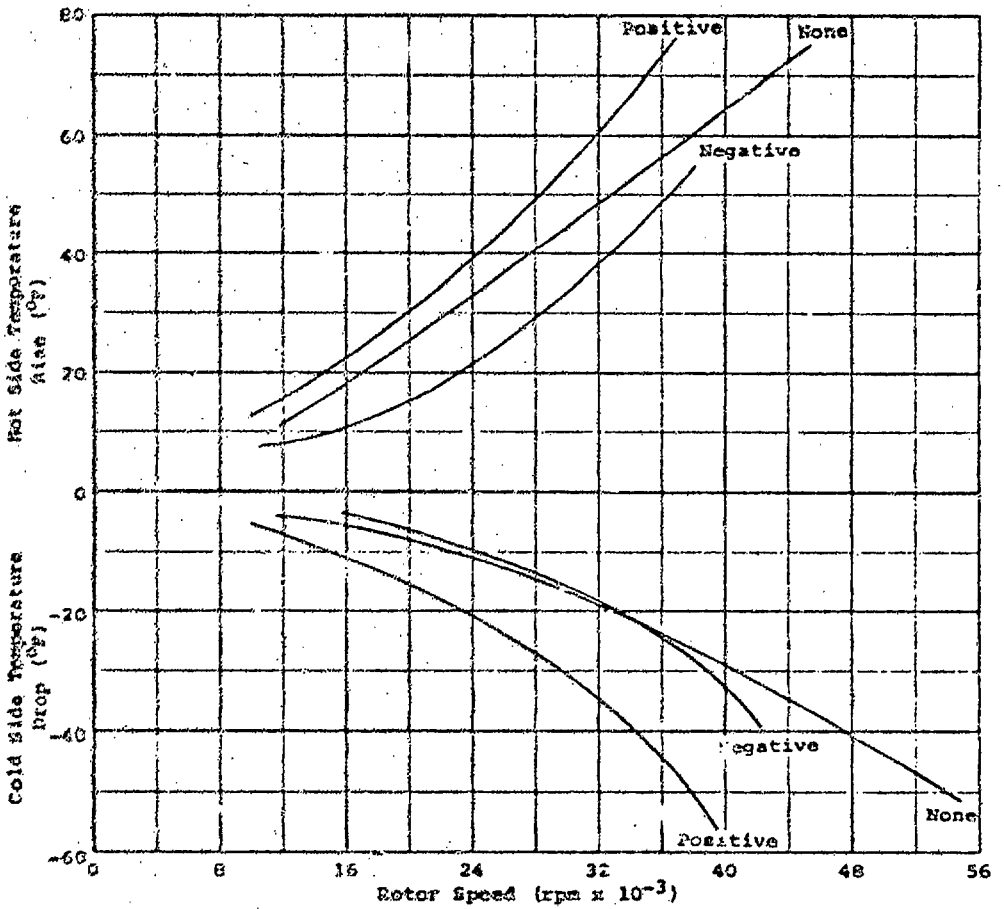

(b) 0.289 Area Ratio

FIGURE 15. A COMPARISON OF THE EFFECT OF PREROTATION ON ENERGY SEPARATION FOR AN FES-3 CONFIGURATION.

Comparison with Theory

The effect of prerotation was suggested by a theoretical investigation of the energy separation phenomenon. In general, theoretical predictions of energy separator performance have been made by establishing a baseline of performance, neglecting bearing friction, prerotation, etc. The effects of these factors were then shown as a modifications of basline performance. Such relationships are graphed in the Foa study[5]. Specifically for Model III, graphs of theoretical baseline performance were available from previous work, showing the actual temperature differential and rotor speed expected for a given inlet/outlet pressure ratio.

In Figure 16, the theoretical temperature increase and decrease are shown versus pressure ratio for the no-prerotation, 0.577 area ratio configuration[6]. A number of experimental data points are also plotted. It will be noted that the cold side temperature drop is very close to ideal performance, while the hot side increase is far from that expected. Graham explains this phenomenon as the effect of a resisting torque such as bearing friction. Energy which would normally have been transferred to the hot output is instead used to overcome the resisting forces. Rough calculations, however, show that this torque must exceed one foot-pound to result in the efficiency loss shown on the graph. Manufacturer's specifications suggest that bearing friction will produce torques less than one-tenth that amount. Furthermore, torques of that magnitude would bring the rotor from 25,000 RPM to rest in a few seconds, a process which in actuality may take several minutes. Thus, factors other than rotor torque must also affect the performance of the device. These

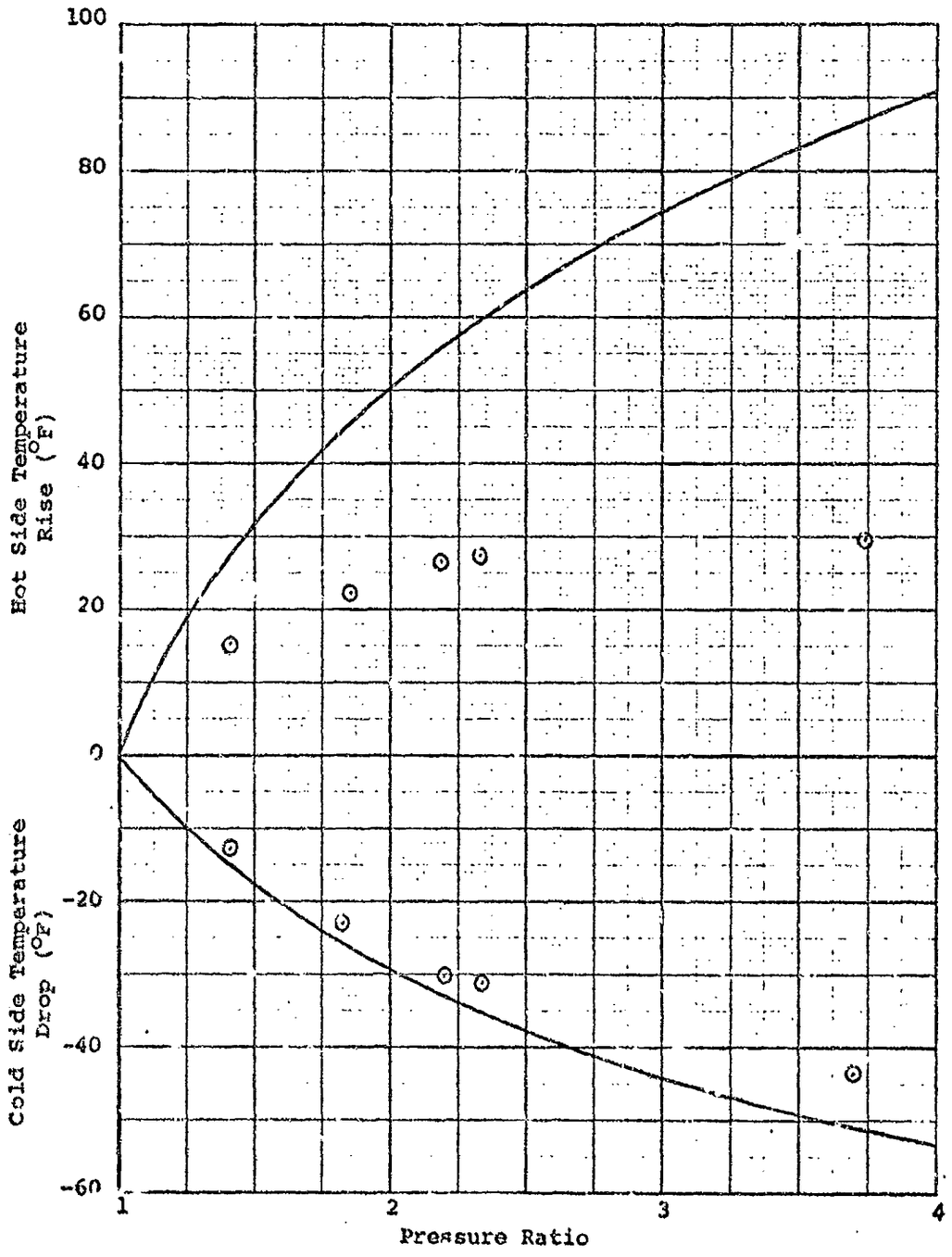

FIGURE 16. THEORETICAL VERSUS EXPERIMENTAL TEMPERATURE CHANGES FOR AN ENERGY SEPARATOR WITH NO PREROTATION AND AREA RATIO 0.577

may include leakage, heat loss to the collectors, and changes in nozzle efficiencies. At higher rotor speeds especially, the nozzle discharge coefficients may have a significant effect on the cold fraction normally determined in internal separation devices by the hot/cold nozzle area ratio.

It is interesting to note (Fig. 17) that for most data points, the rotor speed achieved was equal to the theoretical performance.[6] Furthermore, there is no consistent indication of a back loading effect on rotational speed or on energy separation at a given pressure ratio when the back pressures at both outlet vents are the same. Prerotation, however, does affect rotor speed at a given area and pressure ratio.

Positive prerotation to the cold side definitely enhances performance, despite a reduction in rotor speed. The reduction in speed is, however, desirable in itself if no loss of performance results. Unlike these dramatic effects, back pressure results in no change to either rotational speed or energy transfer at a given pressure ratio. For a given inlet pressure, however, pressure ratio and, therefore, performance are reduced as back pressure increases. The performance at the two area ratios in comparison to theory is shown in Figure 18.

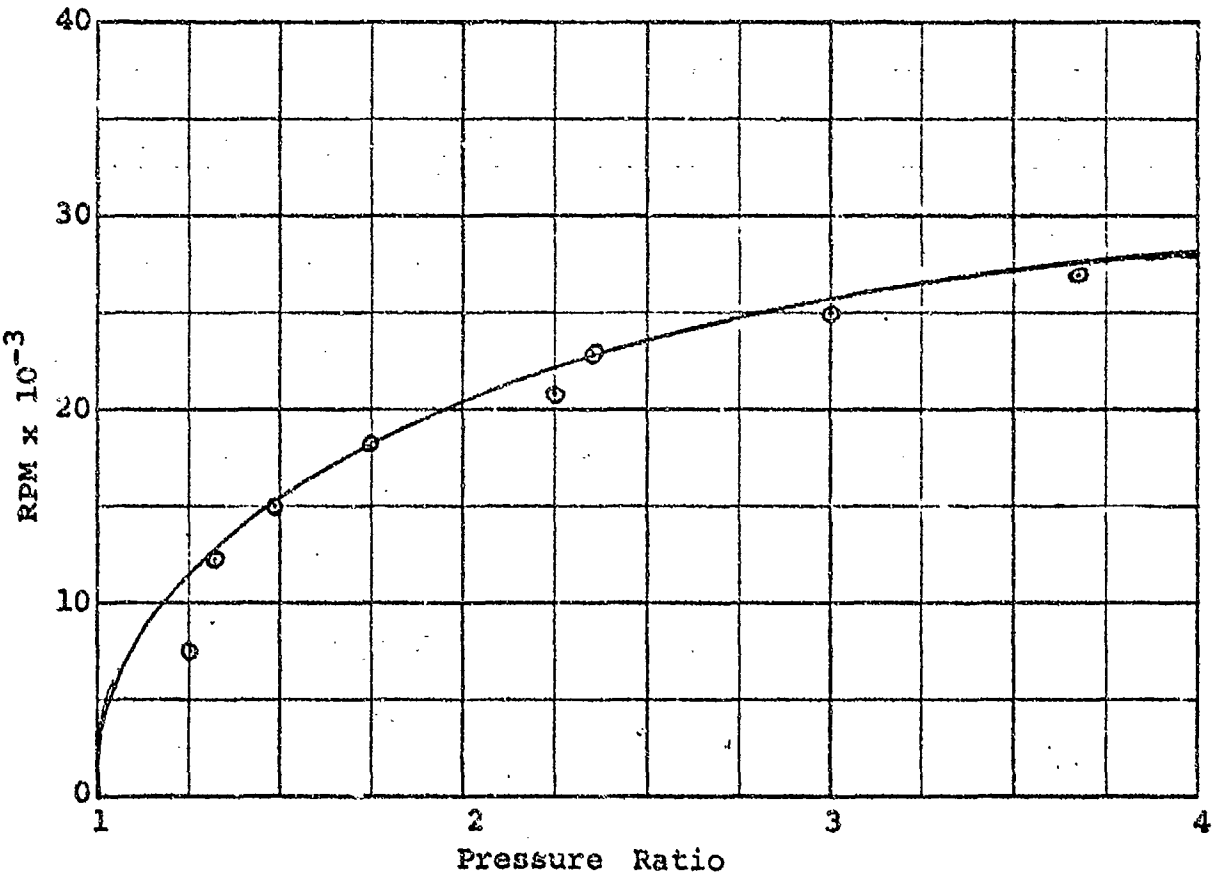

FIGURE 17. THEORETICAL VERSUS ACTUAL ROTOR SPEED FOR FES MODEL III WITH NO PREROTATION AND AREA RATIO 0.577.

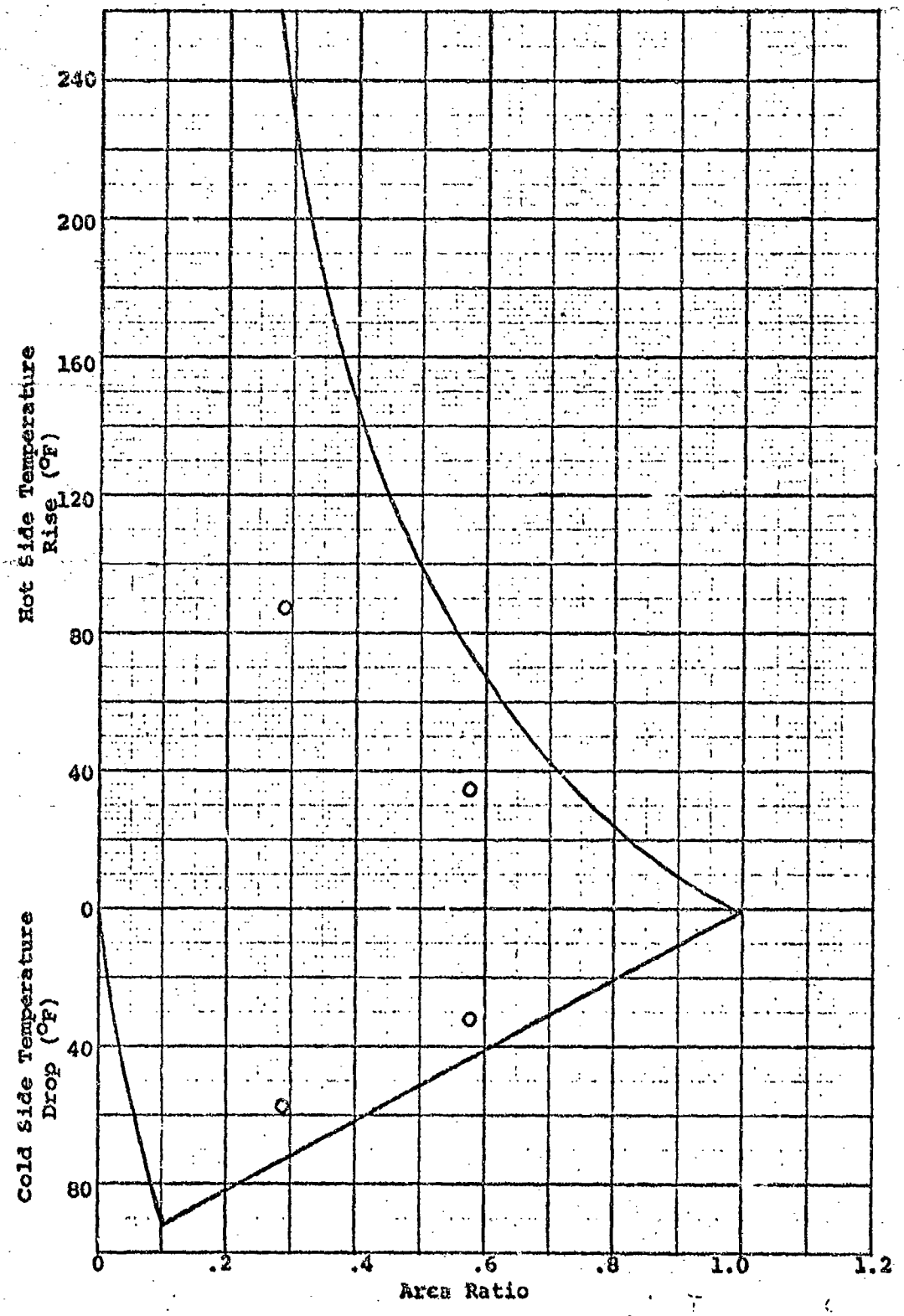

FIGURE 18. THEORETICAL AND EXPERIMENTAL TEMPERATURE CHANGES VERSUS AREA RATIO AT A PRESSURE RATIO OF 3.0.

CONCLUSIONS

This report has discussed an extensive series of tests conducted to investigate the internal version of the Foa Energy Separator. From the results that were obtained, a number of conclusions may be drawn.

1. The ability of an internal separator to operate as an air conditioning device is accurately predicted by Foa's and Graham's theoretical analyses over the range of pressure and area ratios tested. In particular, a decrease in area ratio from 0.577 to 0.289 results in increased cold side temperature drop and rotor velocity at all pressure ratios tested.

2. Operation as a heating device is markedly affected by the operating characteristics of the model such as bearing friction, nozzle geometry, and collector construction. The greatest disparity between theoretical and actual performance is shown in hot side operation; however, in this area lie the greatest possibilities for improved operation of internal separation devices.

3. Energy separator performance can be considerably enhanced through the proper use of prerotation. In particular, inducing an angular velocity in the direction of the cold side rotation can increase energy separation at any of the pressure or area ratios tested.

4. The effect of raising the pressure at both outlets (i.e., back loading the device) is to reduce energy separation at a given inlet pressure. Energy separation at a given pressure ratio is the same, however, at any outlet pressure.

RECOMMENDATIONS

The present work is a significant first step toward the development of alternate means of providing conditioned air for various aircraft applications. Tests have shown that the energy separator concept is feasible at the flow rates required in modern military jets, with cooling capacities limited only by the material properties of the rotor under high speed operation. It is therefore recommended that the energy separator development be continued in a phased program to include:

1. A continuation of the variable geometry internal energy separator test program to evaluate the effects of other prerotation configurations, collector designs, nozzle efficiencies, and unequal back pressures;

2. The design and fabrication of external energy separator models for use in a parametric test program similar to the internal energy separator program;

3. An external energy separator test program. Once completed, the results of this program would be compared to the results of the internal energy separator test program to determine which device offers the most promise for future implementation. This evaluation would consider not only performance, but device construction and compatibility with particular applications;

4. The design, fabrication, and testing of an energy separator for a particular application such as aircraft environmental control or cooling of an onboard oxygen generation system.

REFERENCES

1. Foa, J.V., "Methods of Energy Separation and Apparatus for Carrying Out the Same," U.S. Patent No. 3,361,336, January 2, 1968.

2. Foa, J.V., "Energy Separator," Rensselaer Polytechnic Institute, Troy, New York, Technical Report TR AE6401, January 1964.

3. Graham, P.A., "A Theoretical Study of Fluid Dynamic Energy Separation," The George Washington University, Washington, D.C. Technical Report No. TR-ES-721, June 1972, p. 5-9, 174-203.

4. "A Proposal for Research on a New Method of Energy Separation," The George Washington University, Washington, D.C., October 1970.

5. Foa, J.V., "Performance of the Cryptosteady-Flow Energy Separator," The George Washington University, Washington, D.C. Technical Report No. TR-ES-722, July 1972.

6. Foa, J.V., unpublished notes.

FOA ENERGY SEPARATOR MODEL #3
REDUCED DATA
TABLE 2

Test No.: 1
Date: Oct. 3-6, 1972

Cold Side Precot.: None
Nozzle Area Ratio: 0.577

Inlet/ Back Pressure (PSIG)	RPM	Inlet Flow (lb/min)	ΔT_H (°F)	ΔT_C (°F)	T_i (°F)	U_o (ft/sec)	V (ft/sec)
2/0	7,500	5.84	2.6	1.6	67.2	469.76	82.12
5/0	12,270	10.54	7.2	6.3	65.6	701.45	132.93
5/2	6,600	5.59	2.4	2.1	59.0	531.85	71.51
10/0	17,720	16.13	14.9	14.9	60.8	908.66	191.98
10/2	15,400	14.60	12.6	10.8	50.0	794.70	166.85
10/5	7,100	10.92	3.6	2.5	39.2	620.44	76.92
20/0	23,750	25.40	17.1	30.6	43.7	1,128.79	257.31
20/5	18,000	23.75	15.2	13.6	47.7	935.75	195.01
20/10	19,150	20.95	14.4	12.6	34.8	749.02	207.47
30/0	25,720	31.75	27.0	32.4	59.0	1,276.36	278.65
30/5	20,800	31.11	18.8	24.4	49.2	1,259.33	225.35
30/10	23,340	29.34	17.2	22.5	35.6	980.80	252.87
40/0	27,010	40.64	23.4	42.6	46.4	1,362.74	292.63
40/10	25,750	38.86	26.0	29.8	41.0	1,023.60	278.98
40/20	17,280	36.19	10.0	14.4	49.2	853.72	187.21

FOA VORTEX SEPARATOR MODEL #3
REDUCED DATA

TABLE 3

Test No.: 2 — Cold Side Prerot.: Positive

Date: Oct. 6-12, 1972 — Nozzle Area Ratio: 0.577

Inlet/ Back Pressure (PSIG)	RPM	Inlet Flow (lb/min)	ΔT_H (°F)	ΔT_C (°F)	T_i (°F)	U_o (ft/sec)	V (ft/sec)
2/0	4,460	6.98	3.6	1.8	53.6	463.66	48.32
5/0	9,350	11.43	13.4	8.2	49.2	693.54	102.30
10/0	13,320	16.89	16.2	12.6	46.4	907.54	144.31
10/2	10,150	15.49	9.9	13.5	45.5	795.00	109.97
10/5	5,530	12.12	5.4	1.8	53.6	617.10	59.91
20/0	17,700	21.84	22.4	33.2	37.4	1130.80	191.76
20/2	16,600	26.42	23.5	31.5	42.8	1057.51	179.85
20/5	12,950	24.13	14.4	21.6	44.6	945.05	140.30
30/0	19,880	40.64	28.8	45.0	23.0	1246.35	215.38
30/5	17,000	33.02	23.4	34.2	50.0	1123.53	184.18
30/10	12,950	31.73	13.5	24.3	47.3	969.70	140.40
40/0	18,000	42.80	27.0	46.8	26.6	1343.06	195.01
40/10	17,200	38.48	21.6	25.2	41.0	1176.35	186.35
40/20	12,000	35.83	13.6	12.6	44.6	854.61	130.01

FOA ENERGY SEPARATOR MODEL #3
REDUCED DATA

TABLE 4

Test No.: 3
Date: Oct. 13-16, 1972

Cold Side Prerot: Negative
Nozzle Area Ratio: 0.577

Inlet/ Back Pressure (PSIG)	RPM	Inlet Flow (lb/min)	ΔT_H (^oF)	ΔT_c (^oF)	T_i (^oF)	U_o (ft/sec)	V (ft/sec)
2/0	8,190	6.88	1.8	0	53.6	463.66	88.73
5/0	11,020	12.06	5.4	1.8	46.4	691.66	140.84
5/2	7,180	6.18	2.6	-1.6	57.2	527.58	77.79
10/0	18,000	18.16	11.7	10.8	38.3	900.19	195.01
10/2	13,800	16.70	8.2	2.7	41.0	789.31	149.51
10/5	4,300	10.92	0.9	0	46.4	612.74	46.59
20/0	24,290	25.40	19.9	20.7	47.3	1142.07	263.16
20/2	20,810	25.91	12.6	14.4	39.2	1053.72	225.46
20/5	17,150	25.40	9.9	8.1	38.3	906.17	185.81
20/10	12,660	20.32	5.4	1.8	41.0	742.38	137.16
30/0	27,200	35.18	27.0	27.0	41.0	1269.47	294.69
30/5	23,000	34.67	18.0	18.0	39.2	1111.61	249.19
30/10	17,130	33.02	11.7	9.9	38.3	961.02	185.59
40/0	30,080	44.45	27.9	34.2	44.6	1367.74	325.89
40/10	20,950	41.02	15.4	15.2	41.8	1100.95	226.98
40/20	12,700	38.35	9.0	0.9	37.4	848.32	137.59

FOA ENERGY SEPARATOR MODEL 03
REDUCED DATA

TABLE 5

Test No.: 4
Date: Oct. 17-20, 1972

Cold Side Pretot: None
Nozzle Area Ratio 0.289

Inlet/ Back Pressure (PSIG)	RPM	Inlet Flow (lb/min)	ΔT_H (°F)	ΔT_C (°F)	T_i (°F)	U_o (ft/sec)	V (ft/sec)
5/0	23,030	10.54	27.9	9.9	43.7	809.83	249.51
5/2	11,.50	7.37	9.8	3.6	42.8	520.16	126.22
10/0	31,000	15.24	46.8	19.8	39.2	901.03	335.86
10/2	22,010	13.84	30.6	10.8	39.2	787.92	238.46
10/5	14,000	10.67	16.7	6.3	42.8	610.55	151.68
20/0	40,530	21.59	72.0	32.4	39.2	1132.89	439.11
20/2	35,280	21.34	55.8	19.8	32.6	1046.00	382.23
20/5	32,560	21.21	54.8	18.0	42.8	963.32	352.98
20/10	21,480	19.81	29.2	10.8	46.4	746.40	232.72
30/0	54,750	30.10	83.7	33.1	36.5	1253.74	593.17
30/5	44,380	29.84	60.4	40.4	43.6	1116.34	480.82
30/10	32,860	28.19	46.8	27.0	44.6	967.14	356.01

FOA ENERGY SEPARATOR MODEL #3
REDUCED DATA

TABLE 6

Test No: 5 — Cold Side Prerot: Positive

Date: Oct. 31-Nov. 3, 1972 — Nozzle Area Ratio: 0.289

Inlet/ Back Pressure (PSIG)	RPM	Inlet Flow (lb/min)	ΔT_H ($^{\circ}F$)	ΔT_C ($^{\circ}F$)	T_i ($^{\circ}F$)	U_o (ft/sec)	V (ft/sec)
2/0	9,950	7.19	12.6	5.4	42.8	458.74	107.80
5/0	18,250	10.92	23.4	14.4	39.2	686.72	197.72
5/2	10,130	7.75	12.6	5.8	41.0	519.20	109.75
10/0	30,000	15.24	44.0	30.6	41.0	902.61	325.02
10/2	21,640	14.10	36.0	18.0	35.6	785.08	234.45
10/5	14,900	11.43	11.6	9.0	37.4	607.24	161.43
20/0	38,610	23.24	76.4	52.2	37.4	1,130.79	418.31
20/2	34,300	22.73	68.6	44.0	34.6	1,048.84	371.61
20/5	30,700	22.61	51.0	36.0	35.6	936.54	332.61
20/10	20,400	18.80	32.4	16.2	37.4	739.70	221.02
30/0	41,940	29.46	93.7	65.7	54.5	1,286.50	454.38
30/5	37,850	28.96	81.0	51.3	54.5	1,128.55	410.07
30/10	32,720	28.07	64.8	37.8	53.6	975.73	354.49

PCA ENERGY SEPARATOR MODEL #3
REDUCED DATA

TABLE 7

Test No.: 5
Date: Nov. 3-7, 1972

Cold Side Preset: Negative
Nozzle Area Ratio: 0.289

Inlet/ Back Pressure (PSIG)	RPM	Inlet Flow (lb/min)	T_H (°F)	T_C (°F)	T_I (°F)	U_C (ft/sec)	V (ft/sec)
2/0	10,500	9.40	7.2	0	30.2	452.93	113.76
5/0	20,650	11.18	15.3	6.3	38.3	686.09	223.72
5/2	10,850	8.00	8.0	2.8	40.2	518.81	117.55
10/0	29,100	16.26	28.8	15.4	39.2	901.03	315.27
10/2	23,070	14.48	20.6	9.0	39.2	787.92	249.94
10/5	15,870	12.95	14.4	4.5	36.3	607.80	171.94
20/0	38,350	24.26	53.1	30.6	39.2	1,132.89	415.49
20/2	35,500	21.84	43.2	23.4	39.2	1,053.72	384.61
20/5	31,350	23.50	38.2	16.7	34.3	935.27	339.65
20/10	23,370	21.46	23.4	10.8	35.6	738.40	253.19
30/0	42,400	31.50	63.0	33.6	39.2	1,267.20	459.37
30/5	37,890	31.24	55.3	26.7	34.3	1,106.10	410.51
30/10	33,240	30.73	42.2	20.8	35.6	958.43	360.13

APPENDIX I

REDUCED DATA FROM VARIABLE GEOMETRY ENERGY SEPARATOR TESTS

LEGEND OF SYMBOLS FOR APPENDIX I

RPM= Revolutions of energy separator rotor per minute.

ΔT_h = Hot side output temperature rise above inlet temperature.

ΔT_c = Cold side output temperature drop below inlet temperature.

T_i = Inlet temperature.

U_o = Velocity of nozzle discharge flows, assuming an isentropic expansion from inlet to collector chamber conditions.

V = Velocity of rotor at the periphery.

APPENDIX II

COLUMBIA RESEARCH CORPORATION

TEST FACILITY

In order to provide a facility to test the energy separator developed under this program, Columbia Research Corporation (CRC) has installed sources of both hot and ambient temperature pressurized air (Fig. 19). In addition, systems for the delivery, regulation, and measurement of the air have also been set up. NAVAIR supplied the two primary air sources; a 500 psig compressor and storage tank assembly (Fig. 20); and a small gas turbine (Fig. 21). Since both of these devices were originally built to provide air for starting jet aircraft engines, they have been modified for use as laboratory equipment.

Air Compressor System

The compressor and storage tank unit assembled by Wells Industries provides air at near ambient temperature and up to 500 psig through a 2-inch line to a manifold which currently has three outlets, two of which are regulated. Representative flow rates through the regulators are given in Table 8. The third outlet is at tank pressure and its flow is limited only by the size of the delivery line.

The compressor is a Chicago Pneumatic Model No. PB-43 which handles 8.8 lb/min of air in three stages. Air-to-air radiator cooling is provided after each stage, and the cylinders (four), all on a common crankshaft, are air cooled. (Complete specifications are given in Table 9). It is driven by a 50hp electric motor (440V, 3-phase, 60-cycle) via a belt system designed to permit optimum speeds for both the compressor and motor. Three cylindrical storage tanks with a combined capacity of 335 cubic feet (890 lbs. of air at 500 psig) are fed through a 2-inch diameter line. An automatic control activates the system when the

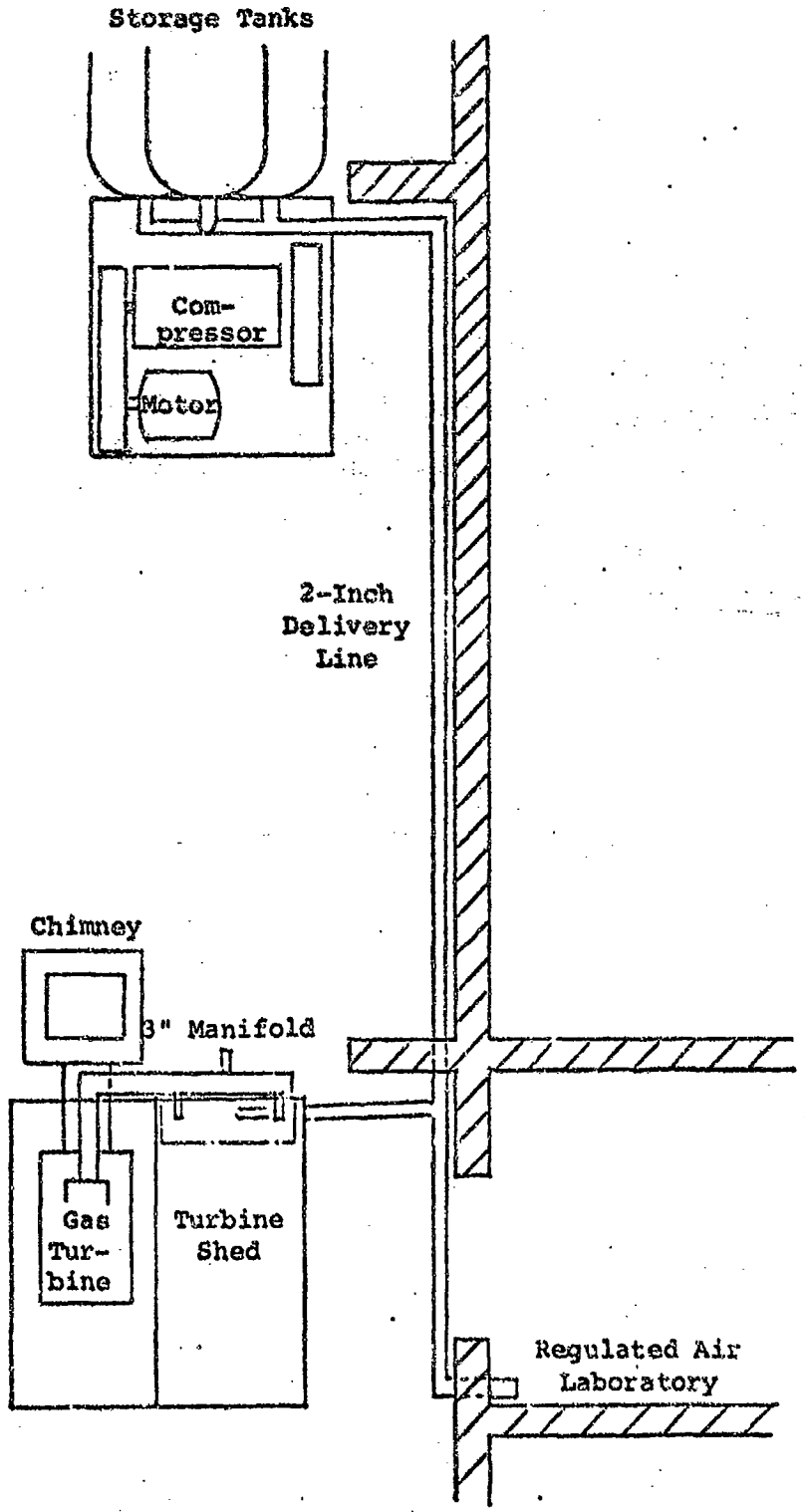

FIGURE 19. COLUMBIA RESEARCH CORPORATION AIR TEST FACILITY.

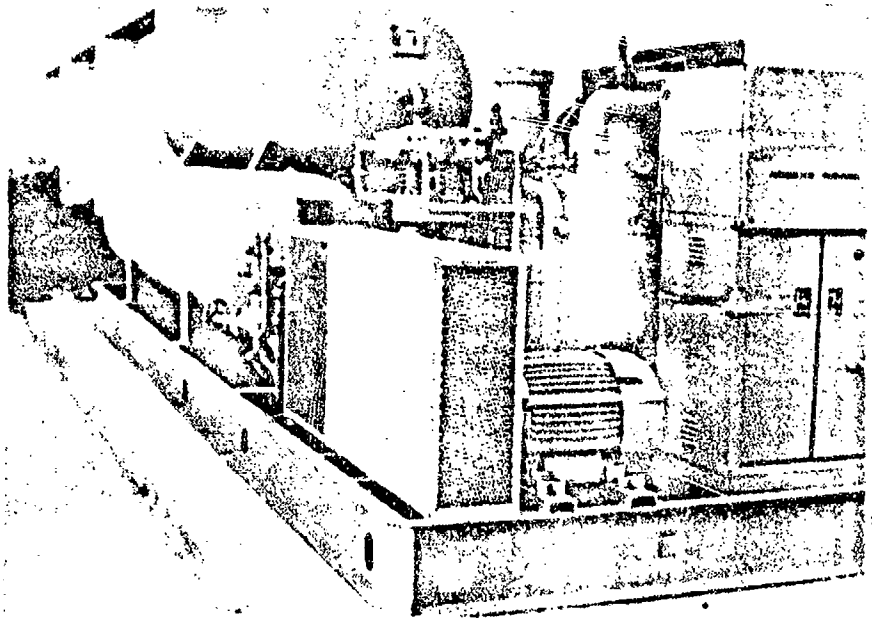

FIGURE 20. 500 PSIG COMPRESSOR.

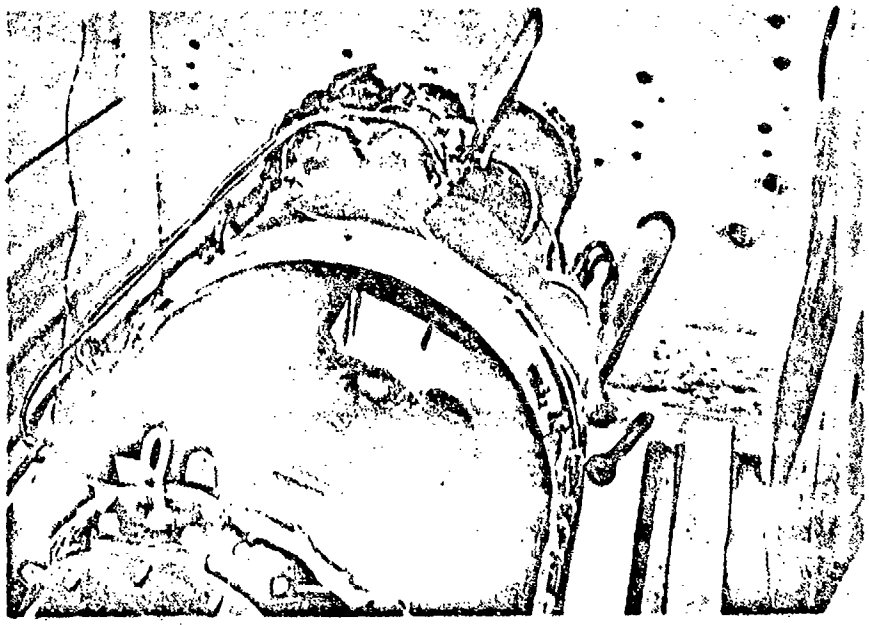

FIGURE 21. GAS TURBINE.

IN STANDARD CUBIC FEET OF AIR PER MINUTE.

Output Pressure PSIG	Receiver Pressure PSIG				
	500	400	300	200	100
50	916	575	338	200	95
75	1000	588	412	238	112
100	675	488	338	212	X
125	738	700	388	238	X
150	781	575	400	225	X
200	700	550	412	X	X
250	775	588	375	X	X
300	600	438	X	X	X
400	612	X	X	X	X
500	X	X	X	X	X

TABLE 8b. FLOW RATES AVAILABLE FROM REGULATOR P-1 IN STANDARD CUBIC FEET OF AIR PER MINUTE.

Output Pressure PSIG	Receiver Pressure PSIG				
	500	400	300	200	100
50	412	325	250	144	88
100	412	325	250	125	X
200	412	319	237	X	X

TABLE 9. COMPRESSOR SPECIFICATIONS

Number of Stages	3
Number of Compressor Cylinders	4
Diameter of Cylinder Bores	8 3/4 - 4 3/4 - 2 1/4 - 2 1/4 Inches
Stroke, Inches	5
Capacity - Compressor Crankcase Oil - Gallons	5
Inlet Pressure, Lb. per Sq. Inch Gauge	0
Discharge Preasure, Lb. per Sq. Inch	500
Pipe Size (Inlet Inches)	3½
Compressor (Discharge Inches)	1
Compressor Speed, r.p.m.	910
Compressor Displacement, c.f.m.	144
Compressor Delivery, c.f.m.	110
Power Required at Belt Wheel, at 500 PSIG Approximate, H.P.	48
Belt Wheel Pitch Diameter, Inches	23 1/8
Number and Size of Belt Grooves	16L
Weight of Compressor	3300
Overall Dimensions (Length)	5'-9"
(Width)	3'-6"
(Height)	5'-3"

tank pressure falls below 450 psi, or a manual override can be used to control both the on-off and compressor loading functions. Venting of the water-oil separator system is also automatic, but CRC has installed an additional manual override.

The laboratory containing the regulator manifold is equipped with a variety of temperature, pressure, and flow rate measuring equipment. These include a direct reading thermocouple thermometer, 1/2-inch and 1-inch diameter primary flow sensing elements, and a number of rotometers, gauges, and manometers. Pipe, tubing, and flexible hoses varying in diameter from 1/8" to 2" are available to deliver air to devices being tested.

Gas Turbine

The Airesearch Corporation gas turbine and related equipment are housed in a shed. The turbine delivers up to 155 lbs/min of air at 75 psig and 540°F from its final compressor stage to a manifold located along the outer wall of the shed. (Complete specifications are given in Table 10.) Two 1-inch diameter ducts return the air to the shed for experimental use, and a third duct provides air for use outside the shed. The flow rate through each of the ducts is independently controllable from a maximum of 70 lbs/min by butterfly valves. The valves are positioned electrically from a control panel (Fig. 22) within the shed. The control panel also monitors turbine operations including RPM, oil pressure, and electric current and voltage.

An instrumentation section (Fig. 23) has been constructed to monitor air flowing through the supply ducts. It contains instruments to measure hot gas temperature, and static and stagnation

Turbine Section

Wheel Type.....Two stage, one radial inward flow, one axial flow
Wheel Governed Speed .....35,141 ± 50 RPM (NOM)
Wheel Governed Speed (no-load).....35,193 to 35,693 RPM
Discharge Temperature

Steady-state Full-load Condition ... 543° ± 8°C (1010° ± 15°F)
Transient Conditions ..... 579° ± 8°C (1075° ± 15°F)

Compressor Sections

Impeller Type .....Two-stage centrifugal
Inlet Temperature ..... 54°C (130°F) (MAX)
Discharge Temperature ..... 302° ± 19°C (577° ± 35°F)

Steady-state Condition with 54°C (130°F) inlet...315°C (600°F) air temperature

Pilot Fuel Control System Fuel Specification - MIL-J-5624, Grade JP4, JP5, or MIL-G-3572 with adjusted performance

Fuel Consumption at Rated Power ..... 367 pounds per hour
Fuel Inlet Pressure ..... 5 PSIG above vapor pressure to 40 PSIG
Fuel Atomizer Cracking Pressure .....75 ± 1 PSIG
Acceleration and Overtemperature Control
Thermostat Setting ..... 574°C (1065°F)

Lubrication System

Oil Specification MIL-L-7808
Oil Pressure .....90 ± 10 PSIG
Oil Temperature .....112° ± 8°C (225° ± 15°F) (MAX)
Oil Pressure Switch Actuation ..... 3 to 5 IN. HG
Oil Tank Capacity.....1.5 gallons (APPROX)
System Residual Capacity ..... 0.25 gallons (APPROX)

Engine Electrical System

Power Supply ..... 26 ± 2V DC
Igniter Plug Type ... High voltage annular surface gap type fired by a condenser discharge unit

Shutoff and Drain Solenoid Valve Solenoid

Operating Voltage ..... 10 to 30V DC
Holding Voltage .....9V DC
Operating Current .....1.5 amperes

Air Scheduling Valve Solenoid

Operating Voltage ..... 10 to 30V DC
Holding Voltage .....9V DC
Operating Current ..... 1.0 amperes

Starter Motor

Rated Voltage .....26 ± 2V DC
Maximum Inrush Current .....750 amperes
Duty Cycle ... 1 MIN on, 4 MIN off with an infinite power source, or unlimited when matched with a battery (#S25210-2)

Ignition Unit

Operating Voltage ..... 14 to 30V DC
Operating Current .....2.5 amperes (MAX)

Centrifugal Switch Actuation

25-percent Switch .....12,300 ± 1000 RPM
95-percent Switch ..... 33,900 ± 600 RPM
Overspeed Switch .....37,400 +100 -400 RPM

Bleed-Air Control System

Differential Pressure Regulator Setting ..... 25 IN. HG
Load Control Air Shutoff Valve Normal Position.....Closed
Load Control Thermostat Setting .. 557° to 560°C (1035° to 1040°F)

Bleed-Air Output with 54°C (130°F) Inlet Air Temperature

Air Flow .....150 pounds per MIN
Air Pressure ..... 72 PSIA

Overall Dimensions

Height ..... 22.0 IN. (APPROX)
Length ..... 56.5 IN. (APPROX)
Width ..... 22.0 IN. (APPROX)
Unit Dry Weight ..... 481 pounds (MAX)

TABLE 10. AIRESEARCH TURBINE SPECIFICATIONS.

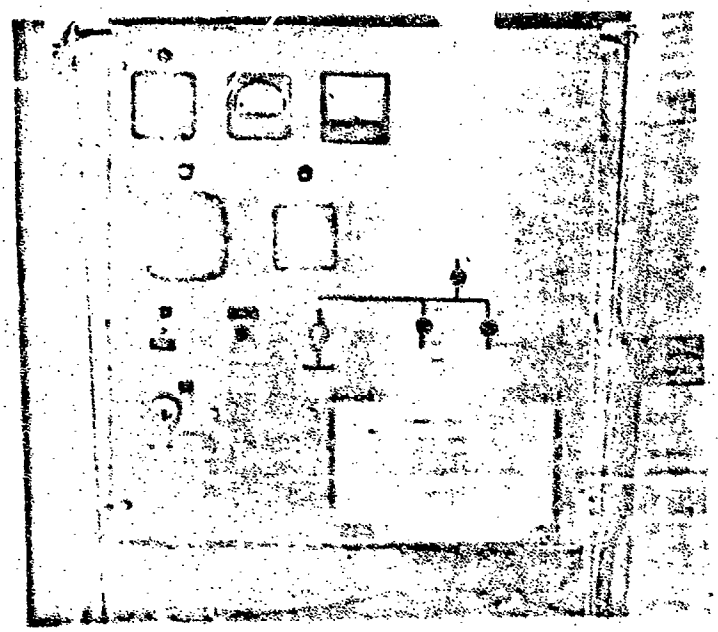

FIGURE 22. TURBINE CONTROL PANEL

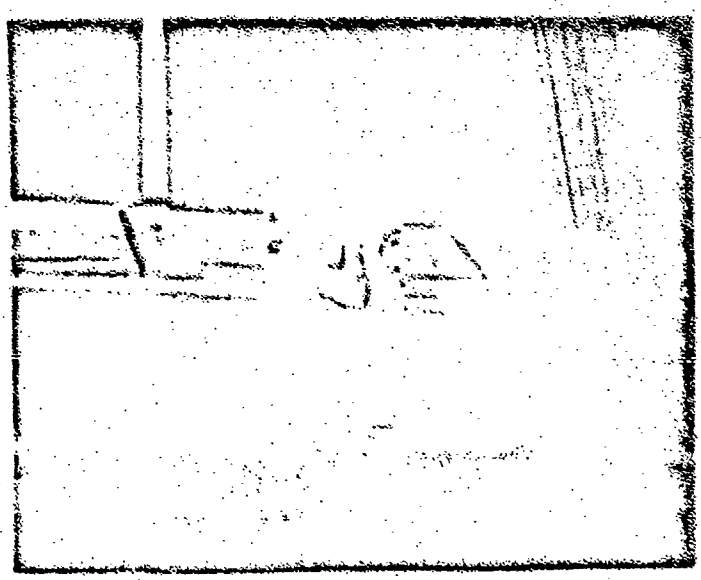

FIGURE 23. INSTRUMENTATION SECTION INSTALLED ON THE OUTSIDE SUPPLY MANIFOLD

pressures, and provides a tap for additional air supplies. Most of the measuring equipment from the regulated air laboratory may also be used in the turbine facility.